An Integrated Decanter Centrifuge-Pitot Pump

M. Farooq Ellahi

Bachelor of Science in Mechanical Engineering
Massachusetts Institute of Technology
May 1994

Submitted to the Department of Mechanical Engineering in Partial Fulfillment of the Requirements for the Degree of

Master of Science

at the
Massachusetts Institute of Technology

May 1996

Signature of Author_____
Department of Mechanical Engineering

Certified by_____
Professor Alexander H. Slocum
Thesis Supervisor

Accepted by_____
Professor Ain A. Sonin
Chairman, Graduate Committee

An Integrated Decanter Centrifuge-Pitot Pump

M. Farooq Ellahi

Submitted to the Department of Mechanical Engineering in Partial Fulfillment of the Requirements for the Degree of Master of Science

Abstract

This thesis first establishes the need for a grinding job shop-affordable, automatic, self-cleaning separator, tailored to remove low specific gravity ceramic fines on the order of 5 microns from water-based coolant in ceramic grinding applications. Next, a design concept is explored, which eventually leads to an integrated decanter centrifuge-pitot pump design. The integrated decanter centrifuge-pitot pump design is shown to be novel and patentable. Calculations based on elementary fluid mechanics are performed to demonstrate that the pitot pump can generate the high pressure flow required by hydrostatic bearings in precision machine tools. The calculations also show that the drag on the pitot tube can be greatly reduced by appropriate selection of pitot tube geometry. Finally, a preliminary design for the integrated decanter centrifuge-pitot pump is presented, based on altering the design of an existing decanter-type centrifuge to accommodate a pitot pump bowl design.

Thesis Supervisor: Dr. Alexander H. Slocum
Title: Alex and Brit d'Arbeloff Associate Professor of Mechanical Engineering

Acknowledgments

First I would like to thank the Naval Research Laboratory for supporting this project. In particular, I would like to thank Dan Gearing, David Armoza, and Lawrence Schuette, the representatives of the Naval Research Laboratory who where involved in monitoring this work and other ongoing projects, for providing the financial support.

I would also like to thank my advisor, Professor Slocum, for his untiring support and guidance. Dr. Slocum also happened to be my thesis advisor for my Bachelor's thesis. Over the years together, he has instilled confidence in me as a designer and made the pursuit of identifying problems and finding creative solutions fun and exciting. For this and more, I am grateful.

Finally I would like to dedicate this thesis to my parents, Afzaal and Lise Ellahi. They have devoted much of their lives in providing me with the best educational opportunities and environments to ensure that I succeed, and have set an example as model parents.

Table of contents

1. Introduction

Self-compensating hydrostatic bearings offer important advantages over other bearing types in machine-tool applications. The HydroGuide™ table-slide linear motion bearings have demonstrated that hydrostatic bearings provide straighter travel, better damping, and greater dynamic stiffness than other bearing types [1]. The Hydrospindle™ has the capability to provide high bi-directional load capacity and stiffness, combined with excellent accuracy and repeatability [2]. Furthermore, self-compensating hydrostatic bearings can have potentially infinite life, provided they are maintained properly. To operate and maintain these bearings properly requires support equipment such as a high pressure pump, filtration and distribution system. This makes the support equipment an integral part of the hydrostatic system.

This thesis was motivated in part by the need to find a filtration solution to separate small ceramic fines of low specific gravity from water-based coolant. Weldon Machine Tool Inc., a company that builds grinding machines that use HydroGuide bearings, found that their filtration system failed to remove abrasive low specific gravity ceramic fines from the water-based coolant going to the hydrostatic bearings. As a first step, a solution was sought after in the filtration literature and relevant publications. Afterwards, suppliers of different types of filters and separators were contacted to provide a cost-effective solution. End-users of filtration equipment involved in ceramic and glass grinding applications were also contacted and asked to comment about their experiences with filtering ceramic fines. It was universally found that centrifugal separation proved to be the most cost-effective means for separating low specific gravity fines from water-based coolant. Chapter 2 summarizes the findings, and discusses the influence of good filtration on the performance of the hydrostatic machine tool system.

From the findings, it was apparent that there was an immediate need for a job shop-affordable, self-cleaning separator dedicated to removing low specific gravity

ceramic fines from water-based coolant. Chapter 3 explores a design concept for the separator, and concludes that the concept had a serious shortcoming. The search for an alternative conceptual design led to an integrated decanter-type centrifuge-pitot pump, which combines the pump and filtration system into one unit. Chapter 4 presents calculations which validate the concept. Chapter 5 presents a preliminary design for the centrifuge-pump, and discusses its novel design features. Chapter 6 presents conclusions and recommendations for further work. To acquaint the reader with filtration basics, Appendix A describes important filtration parameters and their influence on filter performance, and discusses how filter suppliers rate filter efficiency. Appendix B presents a survey comparing the costs and important specifications of different batch-type centrifuges.

2. Establishing the need

With the growing demand for ceramic components, job shops are increasingly grinding ceramic parts. While such job shops often use a different machine tool for grinding ceramic than for grinding metal, they often use the same filtration equipment for both ceramic and metal grinded fine-laden coolant. Such filtration equipment includes settling tanks, cyclonic filters and media-type filters or cartridges. Cyclonic filters have proven to be ineffective at absolutely removing ultra-fine ceramic particles with low specific gravities. Such particles remain in suspension too long, also undermining the use of settling tanks. The long length of time that a small ceramic fine would remain in suspension can be appreciated by considering Stoke's settling velocity equation, valid for $Re << 1$:

$$V_s = \frac{D_p^2 g \Delta\rho}{18\mu} \tag{2.1}$$

where V_S is the settling velocity, D_p is the particle diameter, g is the gravitational acceleration, $\Delta\rho$ is the difference in density between the particle phase and the continuous phase, and μ is the absolute viscosity of the continuous phase. An alumina particle having a spherical shape with a diameter of 5 microns would have a settling velocity of 3.7×10^{-5} m/s in water-based coolant at 20°C. $Re = 6.88 \times 10^{-4}$ which is very much less than unity, so the settling velocity equation is valid. For a three foot deep settling tank, it would take the particle almost seven hours (6 hr. 52 min.) to settle. The accumulation of such fines in the coolant leads to the following undesirable results:

- Change in coolant chemistry, leading to loss of process control
- Decrease in the ability of the coolant to remove heat

- Surface finish deterioration. Contaminants become embedded in the diamond wheel, affecting the surface finish of the part being grinded. This means the wheel has to be dressed more often.

- Abrasion wear. The accumulation of abrasive particles wears precision components such as wetted pump surfaces more rapidly.

While media-type filters have proven to be effective in removing ceramic fines with low specific gravities, they have several drawbacks:

- Recirculating coolant pumped through the filter media, comes in contact with contaminated particles already trapped, and becomes contaminated.

- Coolant that becomes contaminated has to be replaced more often, leading to costly machine downtime, increased cost of coolant disposal and increased cost of coolant replacement.

- Elements that are able to remove small ceramic fines have to be replaced often, leading to high element replacement costs, costly machine downtime and high waste disposal costs.

The need for improved clarification of the coolant going to the grinding wheel goes hand in hand with the need to ensure a continuous supply of clarified coolant to self-compensating hydrostatic bearings. HydroGuide bearings have the advantage that they can use the ceramic grinder's water-based coolant as bearing fluid. This allows cross-talk between the lubrication and coolant systems, meaning only one coolant recirculation system is required. Thus the coolant employed to cool the grinding wheel can also feed

the hydrostatic bearings, which elegantly simplifies the piping system needed. While self-compensating hydrostatic bearings are tolerant to some degree of contamination due to their large bearing gaps, abrasive particles ought to be removed to prevent long-term wear of the wetted bearing surfaces. Such particles are ceramic fines of high surface to mass ratio, which fail to be absolutely removed using conventional filtration means (for metal particles) as discussed above. Thus improved clarification of the coolant has benefits which are multi-fold:

- Coolant chemistry is maintained for improved process control
- Coolant retains maximum heat-removal capability
- Fines are prevented from embedding in the grinding wheel and deteriorating the surface finish
- Minimal abrasion wear of wetted pump parts
- Continuous contaminant-free supply of coolant to the hydrostatic bearings, which results in essentially infinite life

2.1. Centrifugation

At present, small centrifuges with bowls that have to be emptied manually, are the choice of ceramic-grinding job shops that have actively searched for a cost-effective solution to removing low specific gravity fines[1]. Such centrifuges are commonly known as *batch-type* centrifuges. A typical layout for a coolant distribution system incorporating a batch-type centrifuge is shown in **Figure 1**. Fine-laden coolant enters the settling tank above the outlet to the centrifuge. The pump sucks out the concentrated sludge that deposits at the outlet to the centrifuge. Clarified coolant enters from the centrifuge at the other end of the settling tank, and the coolant is pumped out to the machine tool. Occasionally a polishing filter is located downstream of the settling tank to remove remaining fines. In this manner, the batch-type centrifuge continuously clarifies coolant from the settling tank. Affordable batch-type centrifuges have bowls that have to be manually cleaned once they fill up with fines. Typically bowls are cleaned twice per week, for a shop that does production grinding[2].

Automatic, self-cleaning centrifuges are available that will clarify the coolant to cleanliness levels above those desired; however they are prohibitively expensive for the job shop that intends to machine precision ceramic parts. Such centrifuges have several advantages over batch-type centrifuges. The principal advantages are that they can handle larger flow rates, are relatively insensitive to fluctuations in the flow rate, and can maintain constant separation efficiencies (for the meaning of separation efficiency, please refer to section A.1 in Appendix A). Batch-type centrifuges are typically limited to 5-7 gpm optimally, and as the fines fill the bowl, the centripetal acceleration decreases at the outer radius, and thus the separation efficiency decreases.

---

[1]This finding is based on the consensus of opinion of end-users in the ceramic and glass grinding industry contacted by the author, and their filter suppliers.

[2]This finding is based on information from Ferro Ceramics, a production grinding job shop that uses batch-type centrifuges.

Batch-type centrifuges with bowls that have to be cleaned manually, typically cost in the vicinity of $6,000 for a complete system. Appendix B contains further details on the costs and major specification of different batch-type centrifuges. These units can effectively separate flows up to 5 gpm down to 5 microns, using multi-pass closed-loop centrifugation. As the flow rate increases, the bowl size must increase to accommodate the flow. However, there is a limit on how heavy a sludge-laden bowl an operator can lift. For flows greater than 7 gpm, one ought to use an automatic maintenance-free centrifuge or several small centrifuges in concert.

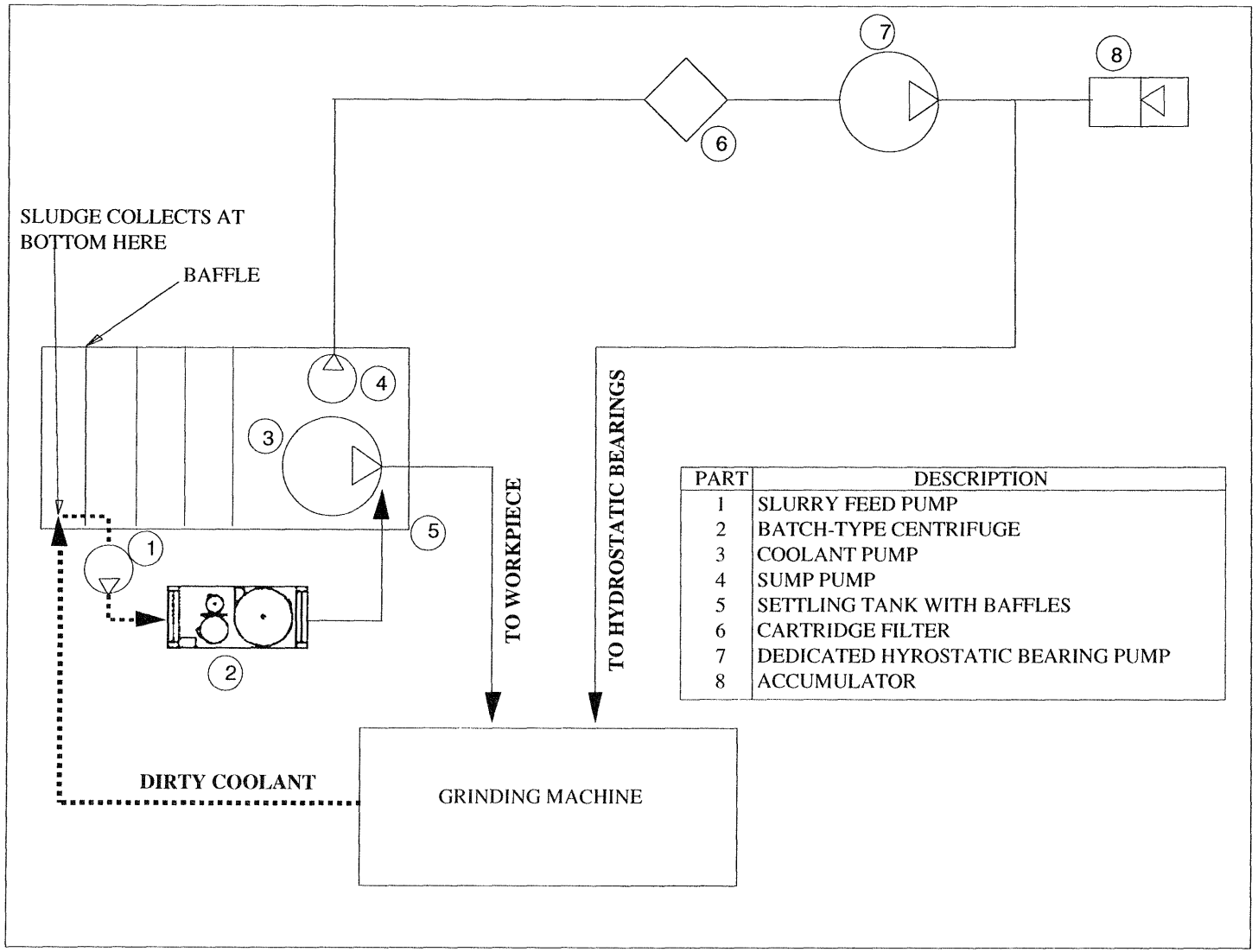

Figure 1: Coolant distribution system incorporating closed-loop centrifugation

3. The Augrifuge

There is a strong motivation to develop an automatic, self-cleaning centrifuge in the same cost range as the small batch-type and with the same processing capability as the small batch-type. This chapter presents a low-cost, automatic centrifuge conceptual design, named the "Augrifuge." The design concept was guided largely by cost-cutting measures, while assuring self-cleaning capability and high performance. An isometric exploded and top view of the Augrifuge is shown in **Figure 2**. **Figure 3** shows a cross-sectional view which illustrates its features. It was conceptualized with the following features:

- No fluid seals to reduce cost and maintenance

- Self-cleaning capability. A screw-conveyor (an auger) moving at a differential speed with the bowl would continually convey the fines out.

- Single drive system. The screw-conveyor could be powered by the drag force of the rotating fluid. Alternatively, the differential speed between the screw conveyor and bowl could be obtained by using a gear system between the spinning bowl and screw conveyor.

- Gravitationally powered injection of slurry and collection of centrate, which eliminates the need for costly pressure fed flow and seals. The slurry would be poured into the screw conveyor's hollow shaft, where it would be accelerated tangentially outwards at the bottom. The centrate would then drain gravitationally through the annular collector, by virtue of the meniscus geometry formed from solid body rotation.

- Abrasion-resistant polymer replaceable liner on inside of bowl. Fines will eventually abrade the inside of the bowl; an abrasion-resistant polymer liner would be fastened to the inside of a steel bowl, to withstand the abrasion from fines-conveying. Once abraded the liner could be replaced with a new one.

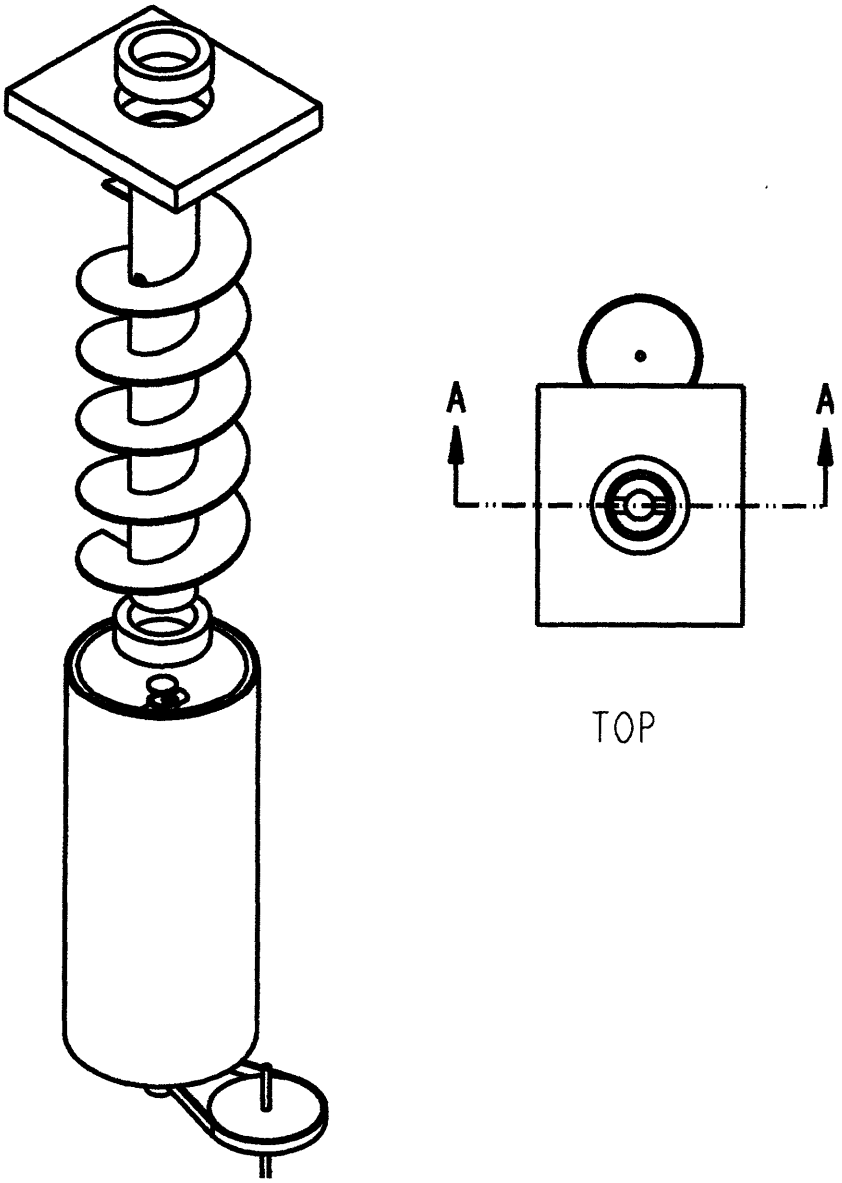

Figure 2: Exploded isometric and top views of the Augrifuge concept

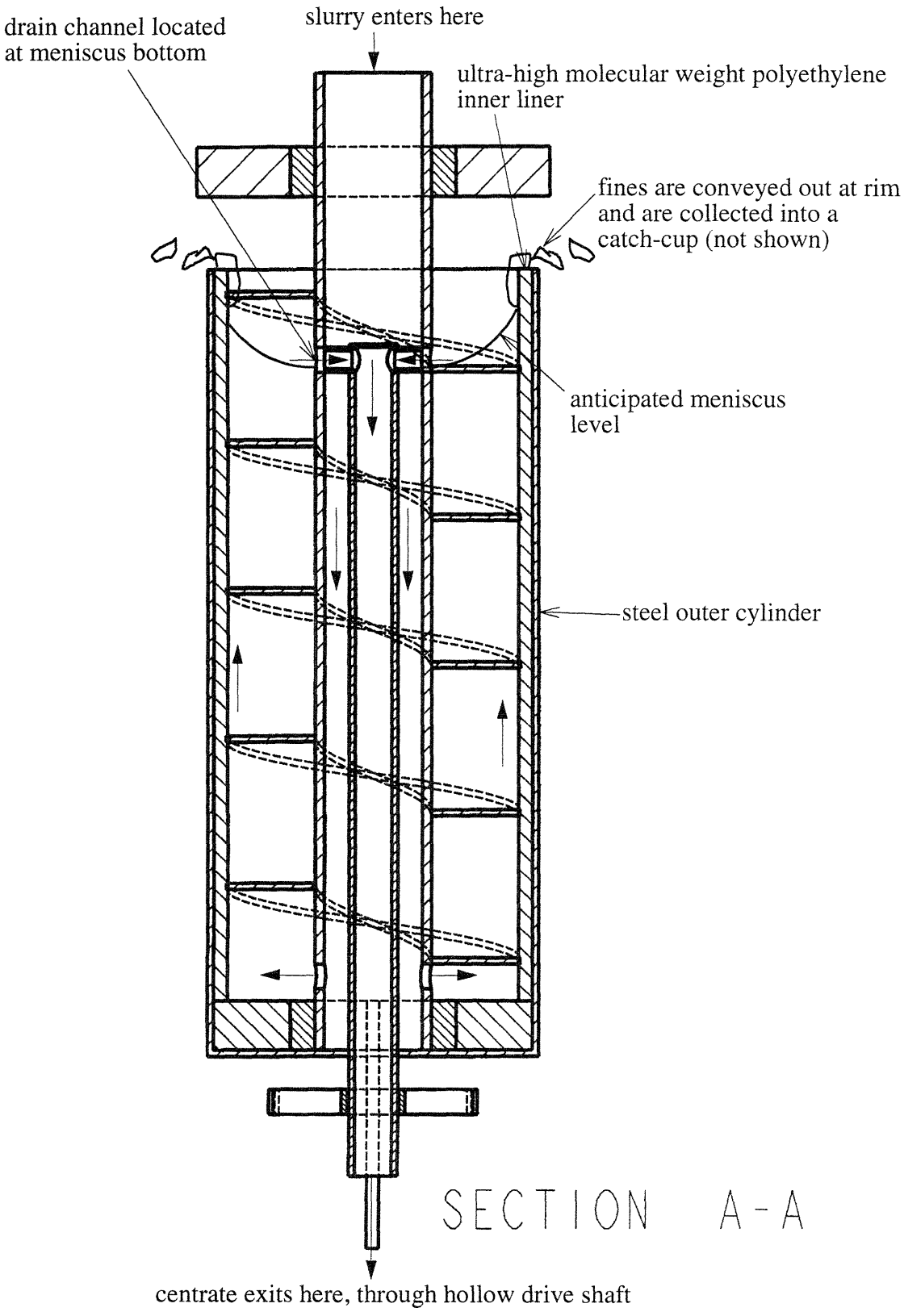

Figure 3: Cross-section showing features and operation of the Augrifuge

3.1. Determination of the fluid free surface geometry necessary for collection

The vertical, open-top design would be greatly simplified if it were possible to collect the centrate at the bottom of the meniscus, formed by virtue of the fluid solid body rotation. The distance from the top to the bottom of the meniscus was thus the determining factor of whether the design would be promising. From fluid mechanics theory, the stagnation gauge pressure is related to the rotational speed ω and radius r from the following relation:

$$p(r) = \frac{\rho\omega^2(r^2 - R_s^2)}{2} + \rho g(h_o - z) \qquad (3.1)$$

where g is the gravitational constant, ρ is the fluid density, and where the remaining parameters are defined by the geometry shown in **Figure 4**. At the free surface, we have the following boundary condition:

$$p(r, z = h) = 0 \qquad (3.2)$$

where h denotes the free surface height. Imposing this boundary condition, and solving for the free surface height h leads to the following:

$$h = \frac{\omega^2\left(r^2 - R_s^2\right)}{2g} + h_o \qquad (3.3)$$

We can find h_O by recognizing that the initial volume of fluid V_1 must equal the volume of fluid at steady state V_2 shown in **Figure 4**, where

$$V_1 = \pi h_i(R_i^2 - R_s^2) \qquad (3.4)$$

$$
\begin{aligned}
V_2 &= \int_{r_s}^{R_i} 2\pi r h dr \\
&= \int_{r_s}^{R_i} 2\pi r \left(h_o + \frac{\omega^2 \left(r^2 - R_s^2 \right)}{2g} \right) dr \\
&= \pi \left[\left(h_o - \frac{\omega^2 R_s^2}{2g} \right) \left(R_i^2 - R_s^2 \right) + \frac{\omega^2}{4g} \left(R_i^4 - R_s^4 \right) \right]
\end{aligned}
\tag{3.5}
$$

Equating V_1 and V_2 and solving for h_O, we obtain

$$
h_o = h_i - \frac{\omega^2 (R_i^2 - R_s^2)}{4g} \tag{3.6}
$$

Substituting h_O into (*3.3*) leads to the following expression for the free surface height as a function of r:

$$
h(r) = \frac{\omega^2 (2r^2 - R_i^2 - R_s^2)}{4g} + h_i \tag{3.7}
$$

The initial height can be obtained by equating the initial state volume with the volume being metered in over the residence time t_r, and solving for the initial height:

$$
h_i = \frac{Q t_r}{\pi \left(R_i^2 - R_s^2 \right)} \tag{3.8}
$$

Here Q is the feed rate.

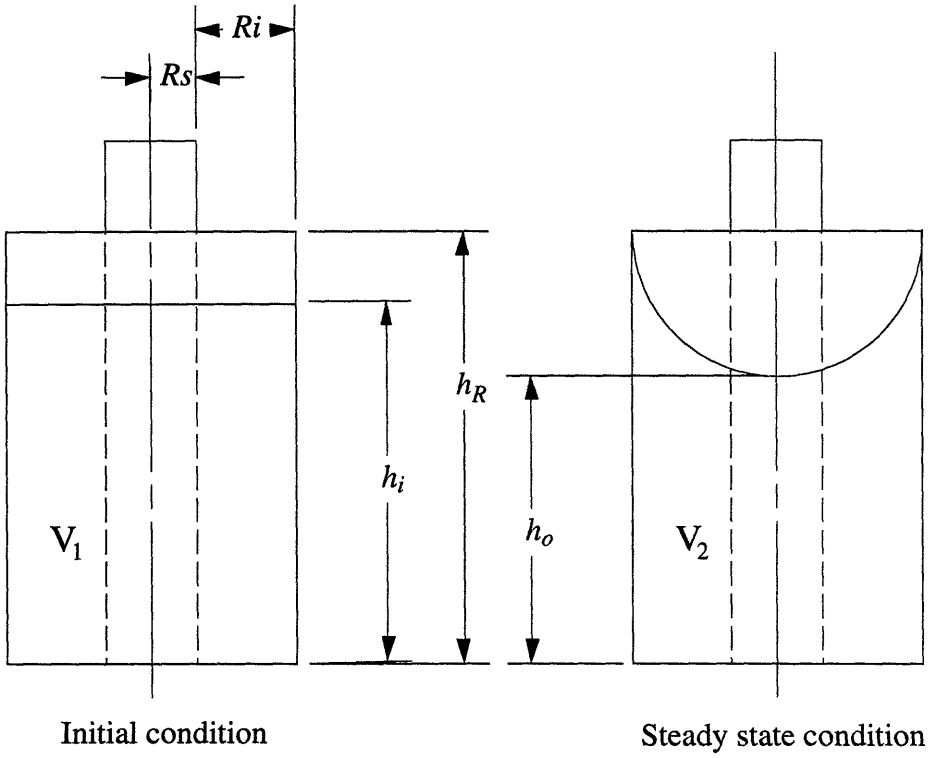

Figure 4: Dimensions for the centrifuge bowl and its contents at rest and in motion

Each of the input parameters was selected as follows:

1. R_i = 3.0". For a first prototype, it was desirable to have a bowl with a radius on the order of 3". Ultra-high molecular weight polyethylene (the most abrasion resistant plastic with zero water absorption) is commonly available in 3" I.D. tubing.

2. ω = 3,600 RPM. A common low-cost motor delivers 3,600 RPM. A 3" radius bowl rotating at 3,600 RPM has an acceleration of 1105 gravities (G) at the 3" radius. In practice, batch-type centrifuges operate at approximately 1000 G, as seen in Appendix B.

3. r_a = 1.1875" - the smallest outer diameter shafting available off-the-shelf for screw conveyors.

4. Q = 1 gpm for pilot testing purposes.

5. t_r = 46 sec. The mean residence time for 6 different batch-type centrifuges surveyed in Appendix B was 23 sec. For the design under consideration, a safety factor of 2 was used to account for any turbulence caused by the auger moving at a differential speed with the fluid.

Results for the free surface height as a function of the radius were calculated by substituting values 1 - 5 into *(3.7)*. **Figure 5** shows the resulting free surface profile. A 6" inside diameter bowl of reasonable height would run dry, since 709" of height would be needed to contain the fluid. The fluid could be contained by covering the centrifuge with a lid. Unfortunately, this would make it impossible to convey out the fines without losing fluid, and the Augrifuge would evolve into a batch-type design. One way to partially reduce the containment height needed, would be to collect at a larger radius, using drain holes that pour into a catch-cup as shown in **Figure 6**. This way of collecting is conceptually similar to the way the centrate is collected in a decanter-type centrifuge, as will be discussed next. However the design still needs a lid to contain the fluid.

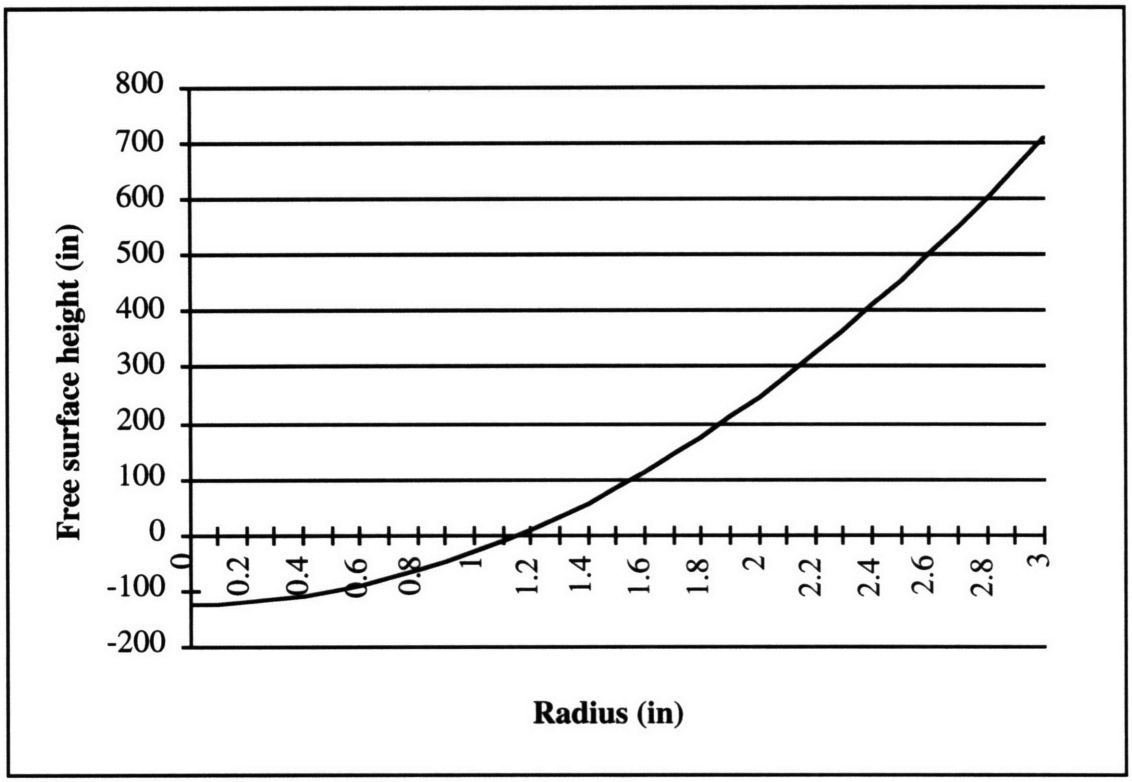

Figure 5: Plot showing free surface height of water as a function of radial position, in a 6" diameter cylinder rotating at 3,600 RPM

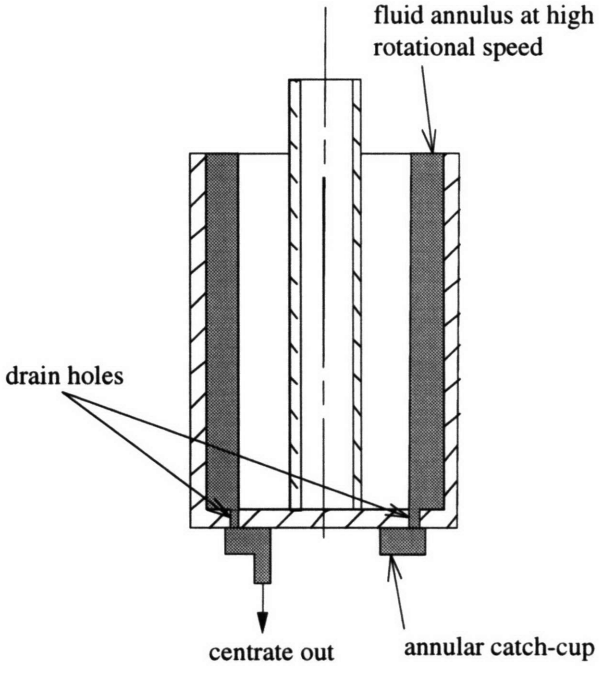

Figure 6: Collection of the centrate using drain holes

3.2. Design of the centrate collector

It is perhaps possible to design a lid and an open-top geometry to allow for solids-conveying, while retaining most of the fluid. At this point however, the designs of successful, automatic self-cleaning centrifuges were carefully examined. The most rugged, and expensive ones are horizontal screw-conveyor type solid bowl centrifuges. They are commonly referred to as *decanter-type centrifuges* or *decanter centrifuges*. Over the past 50 years, decanter-type centrifuge technology has been developed to near perfection. Decanter-type centrifuges are rugged, precision machines dedicated towards separating solids from sludges and slurries primarily in the industrial waste, mining and chemical industries. **Figure 7** shows how a decanter-type centrifuge operates. Slurry enters into the centrifuge bowl through an acceleration chamber, where it is brought up to the speed of the rotating centrifuge bowl. The fines collect along the inner walls and are conveyed through a tapered section to a smaller radius, beneath the level of fluid, where the fines get discharged. The centrate is collected at adjustable weirs, which are similar to the drain holes in the centrate collection system shown in **Figure 6**.

Dr. Slocum observed that if a cylindrical bowl was fastened to the outside end of the centrifuge as shown in **Figure 8**, and the centrate was channeled there as shown, a stationary pitot tube could collect the centrate. The pitot tube would also exploit the high pressure generated by the kinetic energy and the centrifugal force of the rotating fluid, so as to behave as a high pressure, pulsation-free pump. This happened to be the type of pump that was being sought after to power the hydrostatic bearings.

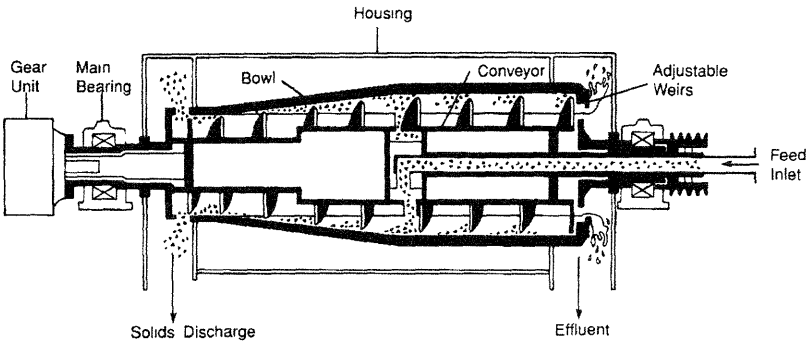

Figure 7: Operation of a decanter-type centrifuge

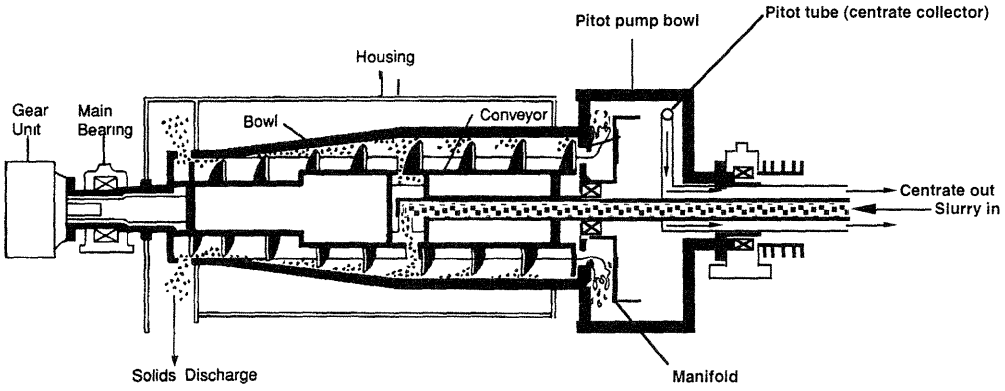

Figure 8: Conceptual design for an integrated decanter-type centrifuge-pitot pump developed in this thesis

4. Preliminary sizing and design of the pitot pump attachment

At present, pitot pumps are commercially available for high pressure, low flow applications. **Figure 9** shows how a state-of-the-art pitot pump operates (courtesy of Enviro-tech Specialty Pumps). The entering fluid is channeled to the inner radius wall of the rotor housing via a manifold. The rotor housing (called *pitot pump bowl* in this thesis) rotates at high speed. The fluid undergoes centripetal acceleration, and jets through the stationary pitot tube to a discharge pipe. **Figure 10** shows pump curves for a family of Roto-Jet® pitot pumps. These pumps can deliver flows up to approximately 450 gpm, pressures up to approximately 2,000 psi, and impart powers on the order of 250 HP. This covers the spectrum of operating points for self-compensating hydrostatic bearings.

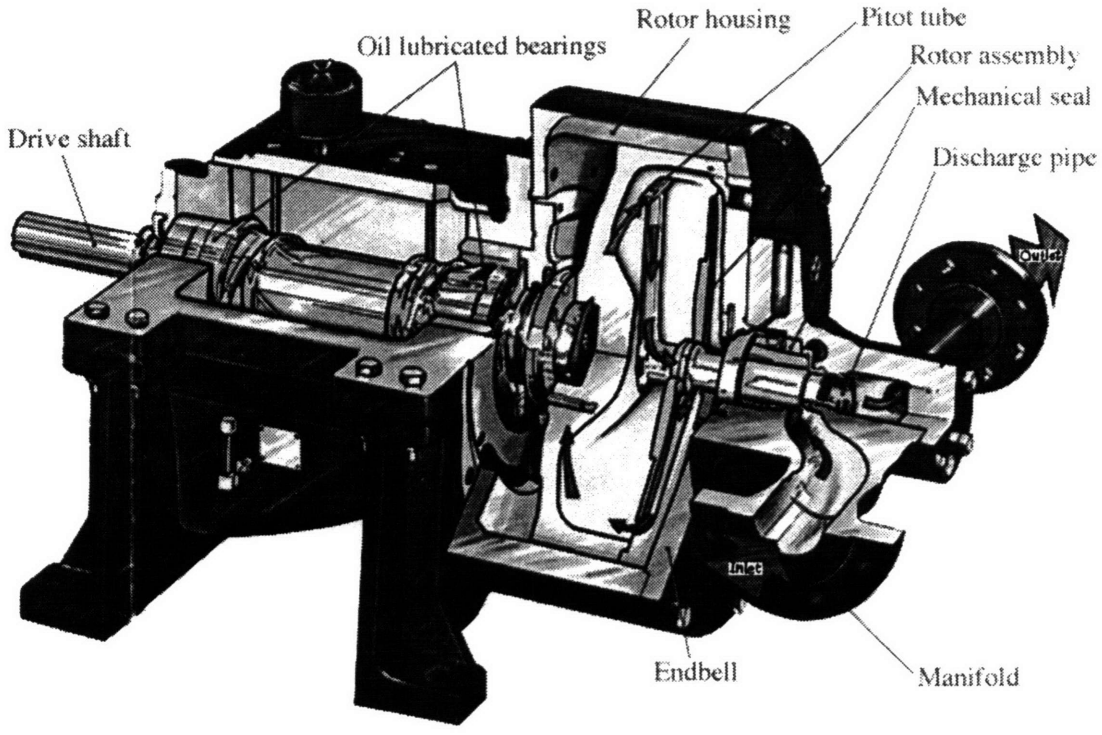

Figure 9: Operation of a state-of-the-art pitot pump (courtesy of Enviro-tech Specialty Pumps)

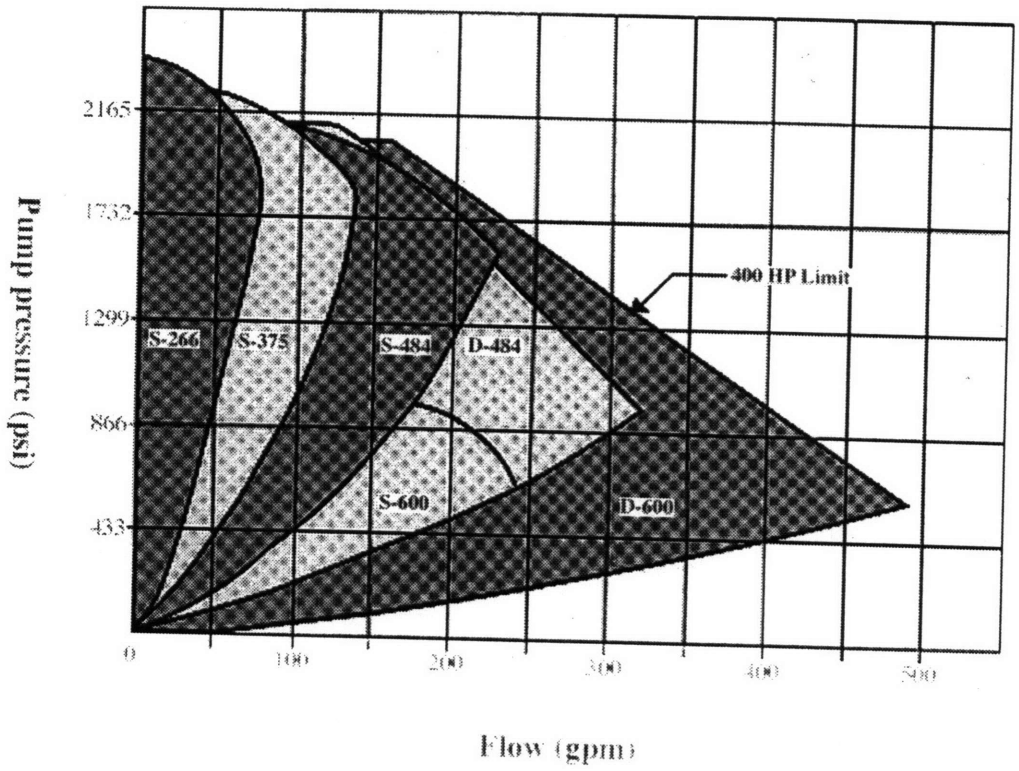

Figure 10: Pump curves for a family of Roto-Jet® series RO pitot pumps (courtesy of Enviro-tech Specialty Pumps)

While the decanter-type centrifuge and the pitot pump are established technologies, the combination of a decanter-type centrifuge and a pitot pump into one unit is a new concept, and a patent for it is in progress. An extensive search of U. S. patents revealed the absence of a machine that combines a decanter-type centrifuge and a pitot pump in the manner described herein. U. S. patent 4,036,427 to Erickson (1977) entitled a "Combination pitot pump and centrifugal separator," discloses a pitot pump which has the separation mechanism within the pitot pump bowl. The separation is accomplished using orifices along the inside radius wall, through which the contaminants are channeled by virtue of the pressure drop across the wall.

U. S. patent 3,279,687 to Amero (1966) entitled "Centrifuge," discloses a decanter-type centrifuge with two or more pitot tubes which are used to scoop the

centrate from the annulus formed within the axial extent of the centrifuge. Here the pitot tubes serve the function of varying the depth of the retained liquid while the separator is running. While Amero recognizes the dynamic pressure build-up at the tube orifice due to the rotating mass of fluid, no provision is made to develop a pitot pump, which has a filled rotating bowl to fully exploit the static pressure build-up of the rotating mass, and a pitot tube with an airfoil-shaped profile to minimize drag losses.

In the conceptual design discussed herein, a pitot pump bowl is designed to deliver a coolant flow rate at the high pressure needed for optimal hydrostatic bearing performance. The pitot pump bowl is fastened onto the centrifuge bowl, so that only one drive is needed to power both bowls, and only one pair of high speed radial bearings is needed for both bowls. It is anticipated that the cost for the integrated centrifuge-pump ends up being on the same order as the cost of the centrifuge alone.

4.1. Analysis of the key design parameters

The goal of the analysis that follows was to determine estimates of two key design parameters for a preliminary pitot pump bowl design, as well as understand the motivation behind having a fully filled pitot pump bowl, and a pitot tube with an airfoil-shaped profile in commerical pitot pumps such as the Roto-Jet pump. Hereinafter, the term "pitot pump bowl" or "pump bowl" refers to the assembly of the pitot pump bowl, pitot tube and discharge pipe through the axial extent of the bowl. The two key design parameters were the following:

1. Pump pressure that can be obtained by retrofitting a pitot pump bowl onto an existing decanter-type centrifuge.

2. Drag force on the tube.

The bowl would eventually be attached onto an existing decanter-type centrifuge. These estimates would indicate whether the concept is feasible. Equations for these design parameters, based on elementary fluid mechanics theory, will be derived in detail next.

4.1.1. Realizable pump pressure

Typically, a supply pressure on the order of 500 psi is sufficient to handle the pressure requirements of a machine tool coolant system integrated with HydroGuide or HydroSpindle bearings. As a first step, it was important to determine whether a pitot pump bowl could generate a static pressure on the order of 500 psi for a 50 gpm flow rate (14.6 HP), when retrofitted onto an existing decanter-type centrifuge.

In commercial pitot pumps, the pitot tube has an aerodynamic shape both externally and internally to minimize drag. For purposes of preliminary design analysis,

however, it was assumed that the pitot tube would be schedule 40 or schedule 80 pipe, having the tubular geometry with two right angle bends as shown in **Figure 11**.

The pressure developed in the pitot tube was determined using Bernoulli's equation. It is important to remark that for this preliminary analysis, internal losses due to friction and bends were neglected. For a streamline from location 1 to location 2 in **Figure 11**, we have:

$$P_1 + \frac{\rho V_1^2}{2} = P_2 + \frac{\rho V_2^2}{2} \tag{4.1}$$

where

$$P_1 = \frac{\rho\omega^2(R_c - R_{fs})}{2} + P_{fs} \tag{4.2}$$

$$V_1 = R_c\omega \tag{4.3}$$

$$V_2 = \frac{Q_p}{A_p} \tag{4.4}$$

$$P_2 = P_p \tag{4.5}$$

Here R_C is the radius of collection, or more precisely the radius at which the center of the pitot orifice is located, R_{fs} is the radius of the free surface of the fluid annulus, P_{fs} is the pressure at the free surface, ω is the rotational bowl speed, Q_p is the desired pitot pump flow rate, P_p is the pitot pump pressure, and A_p is the cross-sectional area of the pitot tube orifice given by the following relation:

$$A_p = \frac{\pi D_p^2}{4} \tag{4.6}$$

Here D_p is the inside diameter of the pitot tube. The first term on the left side of *(4.1)*, P_1, represents the static pressure contribution (by virtue of solid body rotation), and the second term on the left side of *(4.1)*, $\rho V_1^2 / 2$, represents the dynamic pressure contribution. Substituting equations *(4.2)*, *(4.3)*, *(4.4)*, *(4.5)* and *(4.6)* into *(4.1)* leads to the following expression for P_p :

$$P_p = \frac{\rho}{2}\left[\omega^2(2R_c^2 - R_{fs}^2) - \left(\frac{4Q_p}{\pi D_p^2}\right)^2\right] + P_{fs} \qquad (4.7)$$

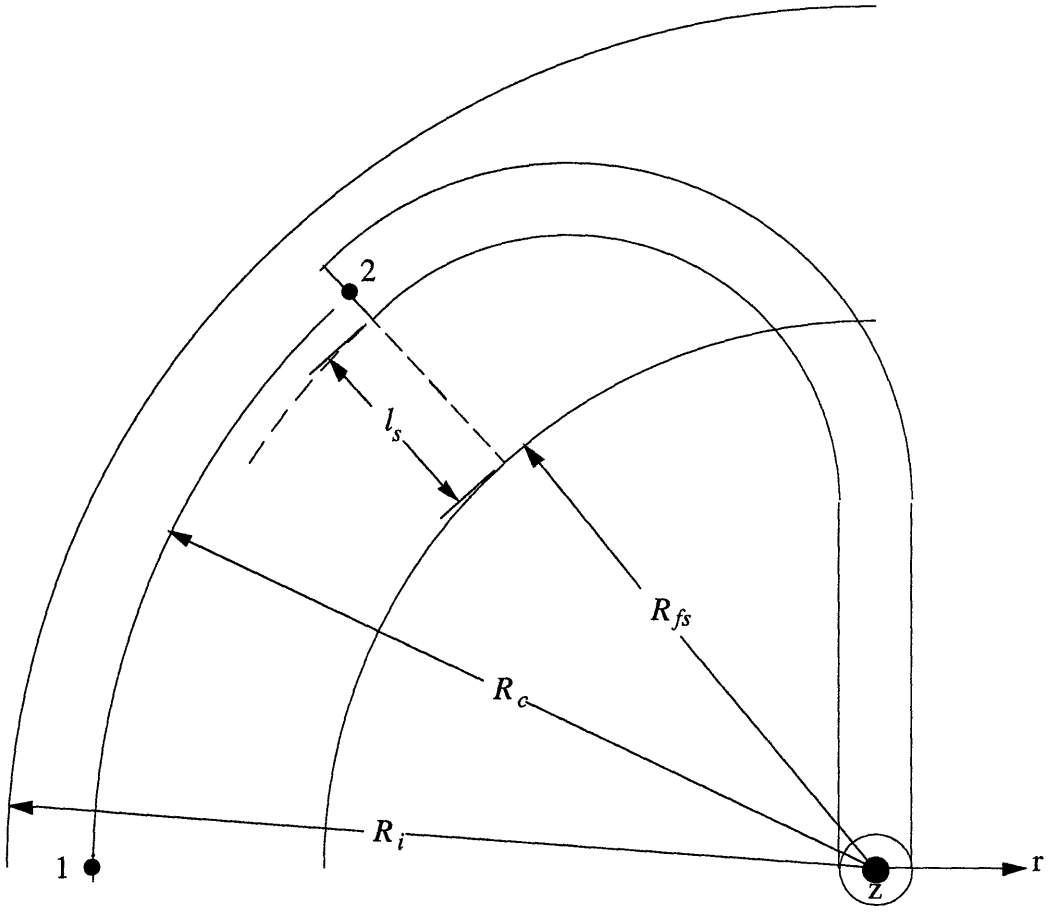

Figure 11: Pitot tube and rotating fluid annulus geometry

4.1.2. Drag force exerted on the pitot tube

At the high operating speeds of the decanter-type centrifuge, the stationary pitot tube would be subjected to a drag force. For the preliminary design, it was important to minimize the drag force. The overall drag force F_D on the pitot tube can be separated into two components:

$$F_D = F_{D_{l_s}} + \rho \overline{V}_{2A_p}^2 A_p \tag{4.8}$$

where $\overline{V}_{2A_p}$ is the average velocity of the fluid over A_p. The first term on the right side of *(4.8)*, $F_{D_{l_s}}$, represents the drag force on the area of tube that is closed to the flow. The area of tube that is closed to the flow is approximately equal to the length of the tube submerged minus the inside radius of the tube, l_S, multiplied by the outside diameter of the pitot tube, D_O. The second term on the right side of *(4.8)* represents the ram-jet force of incoming fluid into the pitot tube orifice (open area). l_S, $\overline{V}_{2A_p}$ and $F_{D_{l_s}}$ are approximated by the following expressions:

$$l_s \approx R_c - \frac{D_p}{2} - R_{fs} \tag{4.9}$$

$$\overline{V}_{2A_p} = \frac{1}{D_p^2}\int_{R_c-0.5D_p}^{R_c+0.5D_p} \omega r D_p dr = \frac{\omega D_p\left(\left(R_c+\frac{D_p}{2}\right)^2 - \left(R_c-\frac{D_p}{2}\right)^2\right)}{2D_p^2} \tag{4.10}$$

$$\begin{aligned} F_{D_{l_s}} &= \frac{\rho C_D}{2}\int_{R_{fs}}^{R_c-0.5D_p} (r\omega)^2 D_o dr \\ &= \frac{\rho\omega^2 D_o\left[\left(R_c-0.5D_p\right)^3 - R_{fs}^3\right]C_D}{6} \end{aligned} \tag{4.11}$$

Here C_D is the tube's drag coefficient.

To compare designs using different pitot tube geometries, it would be worthwhile to develop a parameter that gives a measure of performance based on the drag losses. Taking the fluid volume inside of the pitot pump bowl to be the control volume under analysis, an estimate of the power loss due to drag can be obtained by the following expression:

$$\begin{aligned}\dot{W}_{loss} &= \frac{\rho C_D}{2}\int_{R_{fs}}^{R_c-0.5D_p}(r\omega)^3 D_p dr \\ &= \frac{\rho\omega^3 D_p\left[\left(R_c-0.5D_p\right)^4 - R_{fs}^4\right]C_D}{8}\end{aligned} \qquad (4.12)$$

For this control volume, an expression for a pump drag efficiency η_D can be defined by the following equation:

$$\eta_D = 1-\left(\frac{\dot{W}_{loss}}{Q_p P_p + \dot{W}_{loss}}\right) \qquad (4.13)$$

4.2. Estimation of the key input parameters

Having developed equations for the key design parameters, the next step is to determine appropriate values for the input parameters Q_p, D_p, R_c, R_{fs}, ω, and P_{fs}. Appropriate values were selected as follows:

1. Q_p = 50 gpm. For most machine tool systems that use HydroSpindle and/or HydroGuide bearings, 25 gpm flow is sufficient to supply the bearings. Another 25 gpm flow, at maximum, is needed to cool the workpiece. 50 gpm flow at 500 psi imparts 14.6 HP.

2. The inside diameter of the pitot tube, D_p , had to be optimized such that the pump pressure was maximized, while minimizing drag. For the cylindrical pitot tube, the inside diameter was limited to values available for standard schedule 40 and schedule 80 pipe.

3. The values for R_c and R_{fs} are determined, given the inner radius of the pitot pump bowl. To be conservative, it was assumed that the pitot pump bowl would have the same inner radius as the inner radius of the decanter centrifuge bowl to which the pump bowl would be retrofitted. Bird Machine Company specializes in building decanter-type centrifuges. Bird Machine's model 2500 series decanter-type centrifuges, which typically process 50 gpm, have bowl inner radii of 9". With the bowl inner radius specified, R_c and R_{fs} are the design parameters to be optimized to maximize pump pressure and minimize drag.

4. ω = 3,000 RPM. Bird Machine Company's model 2500 centrifuges have maximum speeds of 3,500 RPM. 3,000 RPM is a reasonable operating speed.

5. $P_{fs} = 0$. There is no internal gauge pressure at the fluid's free surface.

4.3. Preliminary design optimization results

The equations relating the design parameters were entered in an Excel™ Spreadsheet, and optimal values for the undetermined inputs, and key outputs were obtained. **Table 1** summarizes the spreadsheet results, inputs and important constants used to obtain the results for the preliminary design converged on. The design method employed and the graphical results will be discussed in detail next.

Coolant properties			
coolant density		62.4	lbm/ft^3
coolant kinematic viscosity		1.22E-05	ft^2/s
Drag coefficients			
circular tube		0.6	
NACA 0012 airfoil		0.0065	
Inputs			
feed rate	*Qp*	50	gpm
rotational speed	*Omega*	3000	RPM
pump bowl inner radius	*Ri*	9	in
tube tip clearance		0.25	in
pitot tube inside diameter	*Dp*	0.493	in
collection radius	*Rc*	8.4125	in
submerged tube length	*ls*	7.5	in
pitot tube outside diameter	*Do*	0.675	in
pitot tube orifice area	*Ap*	0.19	in^2
ambient gauge pressure	*Pfs*	0	psi
Outputs			
pump pressure	*Pp*	606	psi
drag force exerted on tube	*Fd*	466	lb
pump power imparted	*W*	17.7	HP
pump drag efficiency (cylindrical pitot tube)		15.1	%
pump drag efficiency (airfoil-shaped pitot tube)		94.3	%
free surface radius	*Rfs*	0.675	in
Reynolds number at r=Rfs		8.16E+04	
Reynolds number at r=Rc		1.02E+06	

Table 1: Preliminary design optimization results and values used for coolant properties and drag coefficients

4.3.1. Length of the pitot tube

In order to generate maximum pressure, the pitot tube extended to a radius as close to the inner bowl radius as possible. It was necessary to have some clearance between the end of the tip of the pitot tube and the rotating inner radius wall. For the analysis, a clearance of 0.25" was selected.

4.3.2. Inside diameter of the pitot tube

For the determination of the optimal schedule 40/80 inside pipe diameter, it was assumed that the fluid totally filled the pitot pump bowl, as is true in commercially available pitot pumps. In order to calculate the drag force exerted on the tube using *(4.8)*, it was necessary to select a value for the drag coefficient C_D or find an expression for C_D as a function of Re. Based on the outside pitot tube diameter of 0.675" (3/8" schedule 40 pipe), the Reynolds number computed varied from 8×10^4 at the tube base, to 1×10^6 at the tube tip. **Figure 12** shows the results of Flachsbart, Roshko and Jones and Walker [3] for C_D for flow past a circular cylinder in this range of Re. C_D varies from approximately 1.2 to 0.2, and then levels off between 0.5 and 0.7. There is a transition to higher C_D (~0.5-0.7) in the Reynolds range predicted for flow about the past the pitot tube. It is unclear whether the pitot tube's C_D would obey the empirical curve of **Figure 12**, since the velocity of the flow past the pitot tube varies significantly from tube base to tube tip. For the analysis, C_D was chosen to be 0.6. If the flow had a higher Reynolds number than predicted, then using $C_D = 0.6$ would be a good choice. On the other hand, if C_D varied along the pitot tube length according to **Figure 12**, then using $C_D = 0.6$ would still yield a conservative estimate for the drag force.

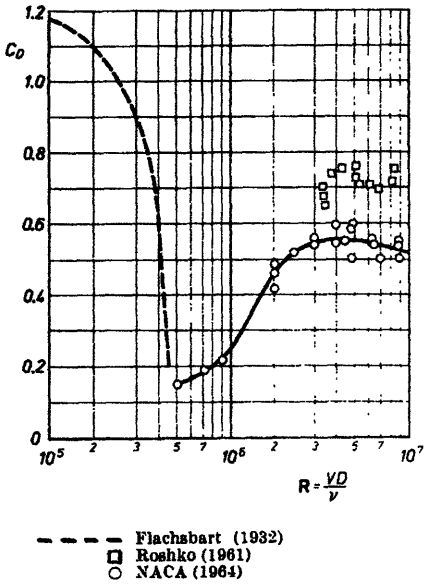

Figure 12: Drag coefficient for flow past a circular cylinder as a function of Reynolds number [3]

Figure 13 shows the influence of schedule 40/80 inside pipe diameter on the total drag, calculated using C_D = 0.6 in *(4.11)*. **Figure 14** shows the influence of schedule 40/80 inside pipe diameter on the pump pressure, calculated using *(4.7)*. **Figure 13** indicates that the drag keeps increasing almost linearly with increasing inside pipe diameter. **Figure 14** shows that for schedule 40/80 inside pipe diameters greater than 0.493", the pressure increases little, which makes 0.493" (3/8" schedule 40 pipe) the optimal choice inside pipe diameter. Hereinafter, values for the inside and outside diameters of 3/8" schedule 40 pipe were used in the calculations.

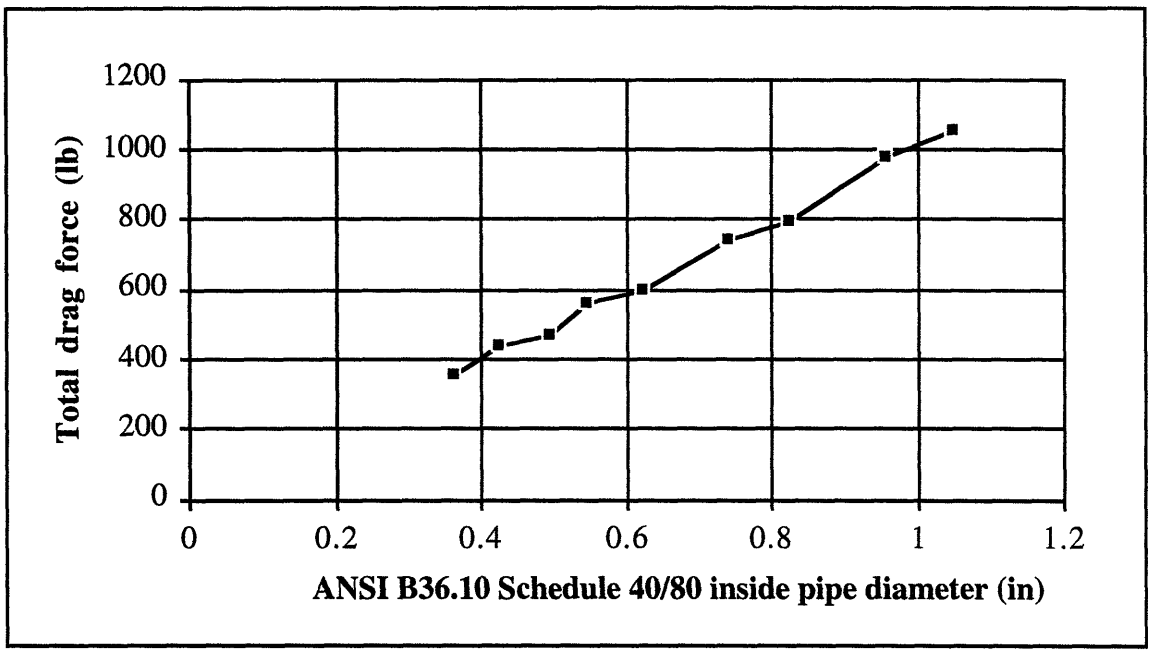

Figure 13: Influence of the inside pipe diameter on the total drag force exerted on the pitot tube for a filled 18" diameter pitot pump bowl rotating at 3,000 RPM

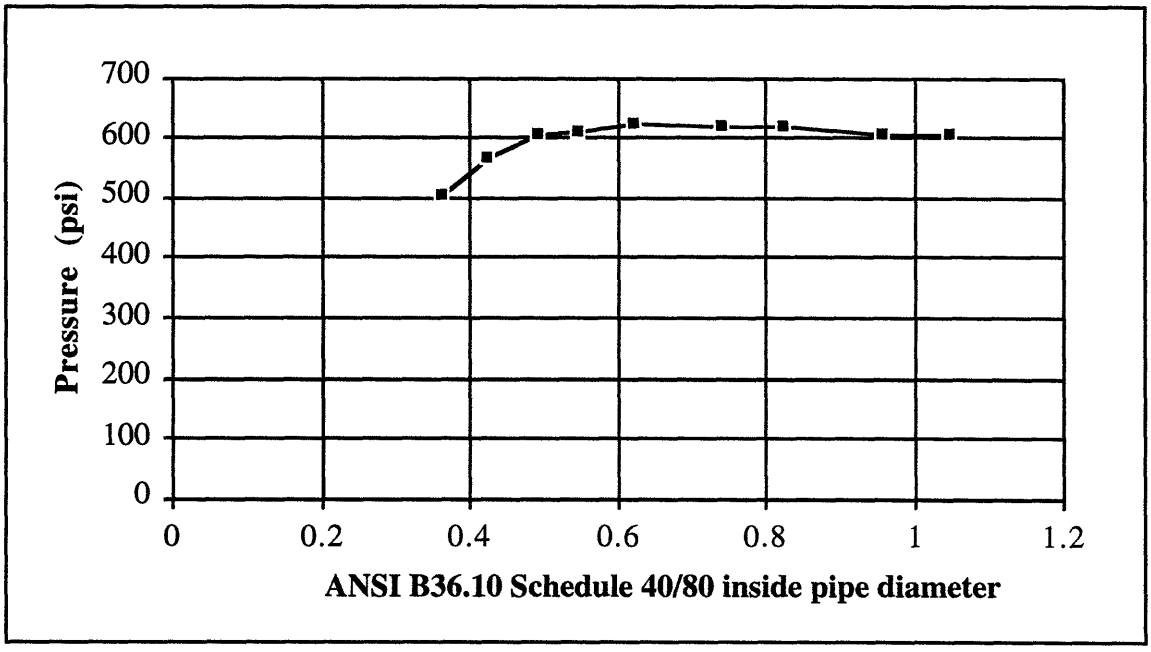

Figure 14: Influence of the inside pipe diameter on the pump pressure for a filled 18" diameter pitot pump bowl rotating at 3,000 RPM

4.3.3. Length of pitot tube submerged

The length of closed pitot tube submerged, l_S (l_S does not include the pitot orifice, which is called "open pitot tube"), determines the location of the free surface radius R_{fS}, or vice versa. Here l_S was optimized, since it is easier to visualize. For the preliminary design, l_S was selected to be 7.5", to maximize pump pressure. A submerged tube length of 7.5" corresponds to a pump bowl that is completely filled. The discharge pipe through which the fluid is pumped to the outside was assumed to have an outside diameter twice the diameter of the pitot tube to allow for some diffusion to a lower flow velocity. Thus R_{fS} (taken along the axial extent of the discharge pipe) was 0.675" for a filled pump bowl (l_S = 7.5"). **Figure 15** shows the influence of l_S on both the drag force on the pitot tube and the pump pressure, for a 3/8" schedule 40 tube (corresponding to an inside pipe diameter D_p = 0.493"). For both results, *(4.9)* was rearranged to solve for R_{fS} in terms of l_S (R_{fS} (l_S)). The results for the drag as a function of l_S could then be obtained by substituting R_{fS} (l_S) into *(4.11)*. Similarly, the results for the pump pressure as a function of l_S could be obtained by substituting R_{fS} (l_S) into *(4.7)*. **Figure 15** shows that as l_S increases, both the pressure and drag increase, but the increase for both pressure and drag diminishes with increasing submerged tube length. At l_S = 7.5", the pump pressure is maximized at 606 psi.

Figure 15 shows that at l_S = 7.5", the drag force is also at a maximum of 466 lb. Fortunately the drag force can be greatly reduced by using a tube that has an airfoil shape. The reason for this, is that the total drag is largely dominated by drag on l_S . **Figure 16** shows the relative magnitudes of the drag components vs. rotational speed for a filled pitot pump bowl (l_S = 7.5"), calculated using *(4.8)*. At 3,000 RPM, the drag on l_S is 2.7 times as large as the ram-jet force on the open pitot tube (pitot tube orifice). Thus, reducing the drag coefficient by using an airfoil-shaped pitot tube, can significantly reduce the drag force.

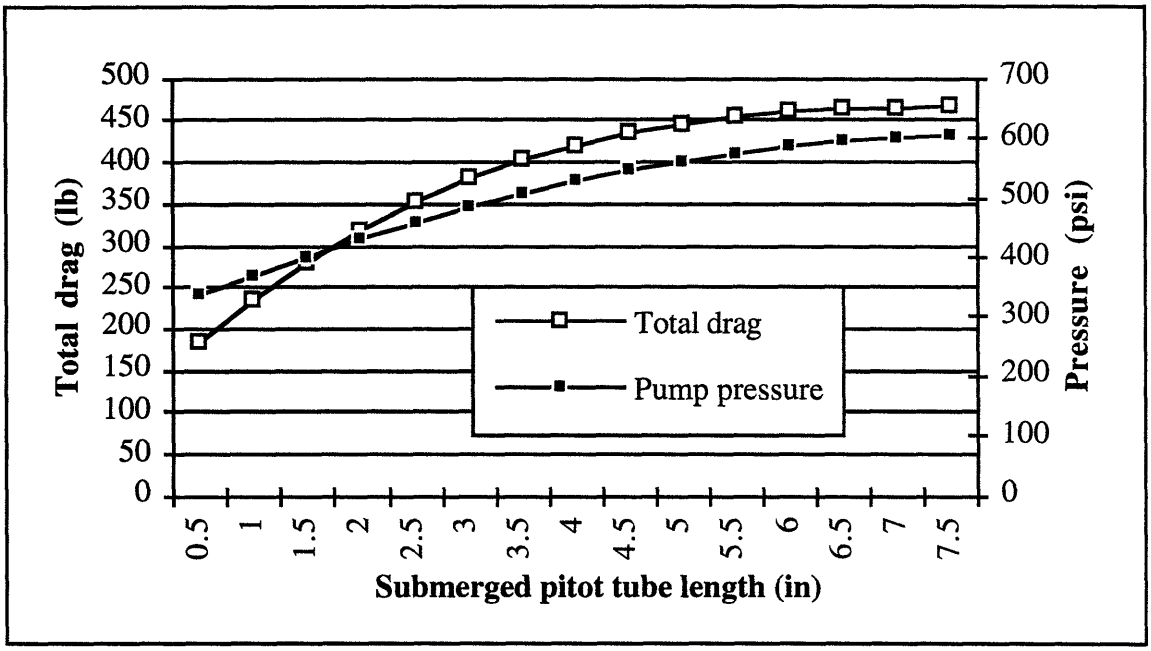

Figure 15: Influence of the submerged pitot tube length on the total drag force exerted on the tube and on the pump pressure generated in the tube, for a 3/8" schedule 40 pitot tube submerged in an 18" diameter pitot pump bowl rotating at 3,000 RPM

Figure 17 shows a graph of the minimum section drag coefficient vs. Reynolds number for several airfoils [4]. To gain an order of magnitude estimate of how much the drag can be lowered by using an airfoil shape, consider the drag characteristics of the symmetric NACA 0012 airfoil. **Figure 18** shows the NACA 0012 airfoil shape [4]. For this airfoil, the minimum drag coefficient varies from roughly 0.010 at Re=2 x 10^5 to 0.006 at Re=9 x 10^6, as shown in **Figure 17**. Given that the drag coefficient for a cylindrical tube is on the order of 0.6 for this Reynolds number range (as discussed above), the drag on the pitot tube can be reduced by a factor of 100 or two orders of magnitude, by going from a cylindrical pitot tube to a pitot tube having an airfoil-shaped profile.

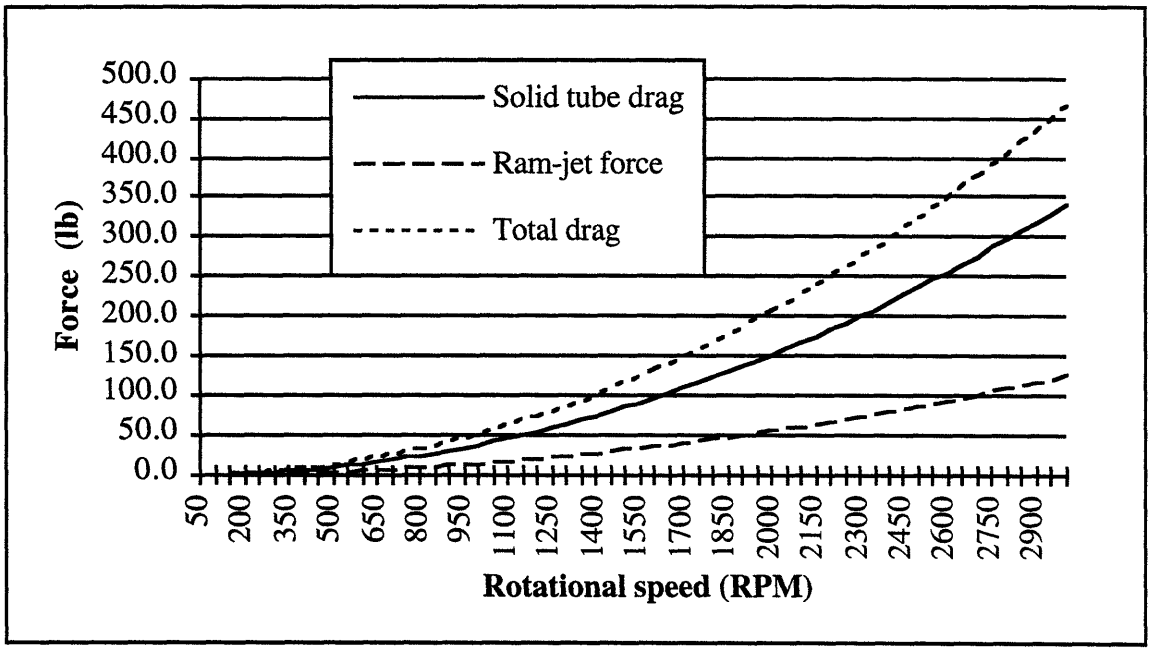

Figure 16: Influence of the rotational speed on the two drag components: solid tube drag, and ram-jet force on the tube orifice. Here the pitot pump bowl is filled (l_S = *7.5"*) and the tube is 3/8" schedule 40 pipe.

The savings in power consumption by using an airfoil-shaped tube rather than a cylindrical tube can be appreciated by graphing the pitot pump bowl drag efficiency (as defined in *4.13*) for the two geometries as a function of the rotational speed, as shown in **Figure 19**. The drag efficiency for the NACA 0012 airfoil shape varies from 94.3 % to 96.2 %, assuming the airfoil's width is equal to the diameter of 3/8" schedule 40 pipe, and assuming C_D = 0.0065 for the airfoil (C_D ~ 0.0065 over much of the Reynolds number range of operation for the NACA 0012 airfoil, as shown in **Figure 17**). For 3/8" schedule 40 pipe, the drag efficiency varies from 15.1 % to 21.5 %, which is quite low. For both geometries, the drag efficiency diminishes with increasing rotational speed. However, this trend is more pronounced for the circular shape than it is for the airfoil shape.

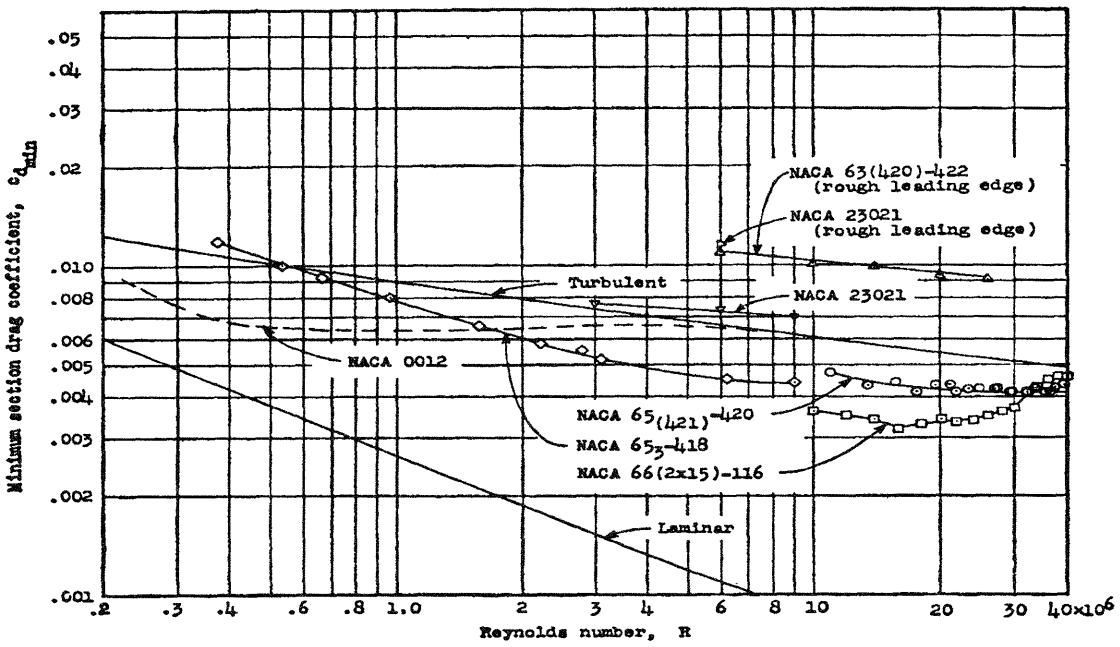

Figure 17: Variation of the minimum drag coefficient with Reynolds number for flow past several different NACA airfoils [4]

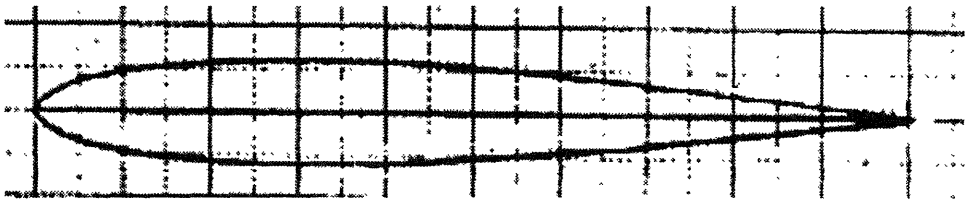

Figure 18: NACA 0012 airfoil shape [4]

Figure 20 shows the dynamic and static pressure contributions to the pump (pitot static) pressure of equation (*4.1*) as a function of the rotational speed, for a filled pitot pump bowl (l_S = 7.5"). Both pressure contributions are equal for a filled pitot pump bowl. The pitot pump flow rate was set at 50 gpm for the optimizations. The pitot tube was thus assumed to have a dynamic pressure of 47.5 psi, by virtue of the 50 gpm flow rate through it. At rotational speeds above 1,150 RPM, the dynamic and static pressure contributions are each greater than 47.5 psi, and the pitot tube becomes a pressure source.

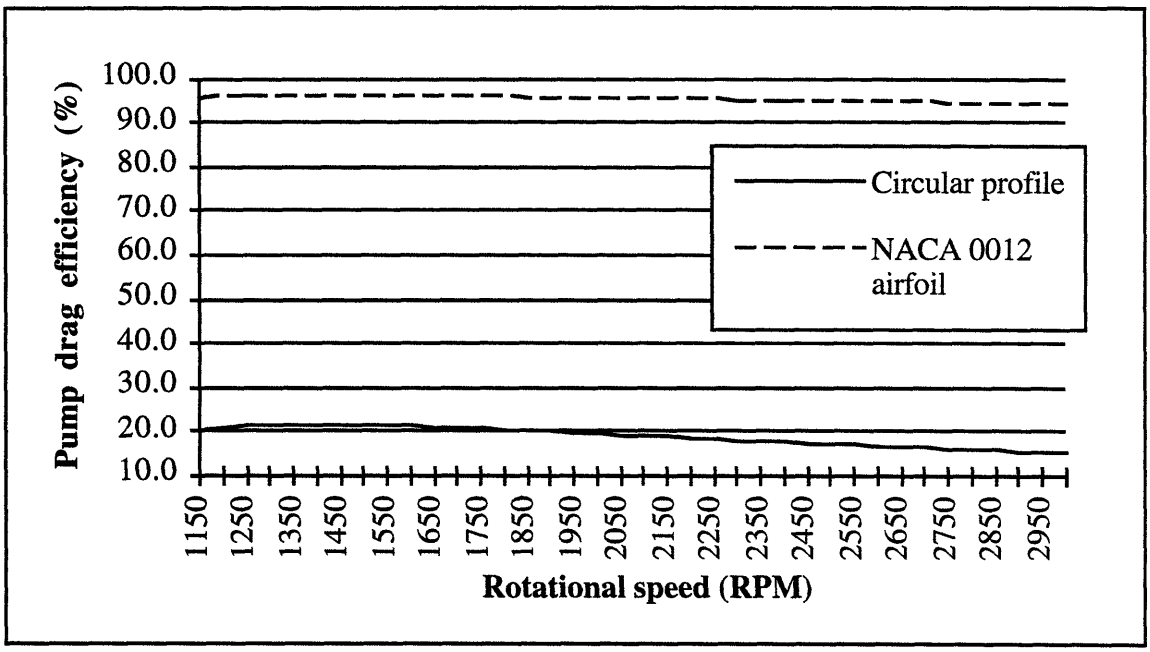

Figure 19: Influence of the rotational speed on the pitot pump bowl drag efficiency (for the definition, see *4.13*) for a 3/8" schedule 40 pitot tube, and a NACA 0012 symmetric airfoil pitot tube having a width equal to the diameter of 3/8" schedule 40 pipe. Here the pitot pump bowl is filled (l_S = *7.5"*).

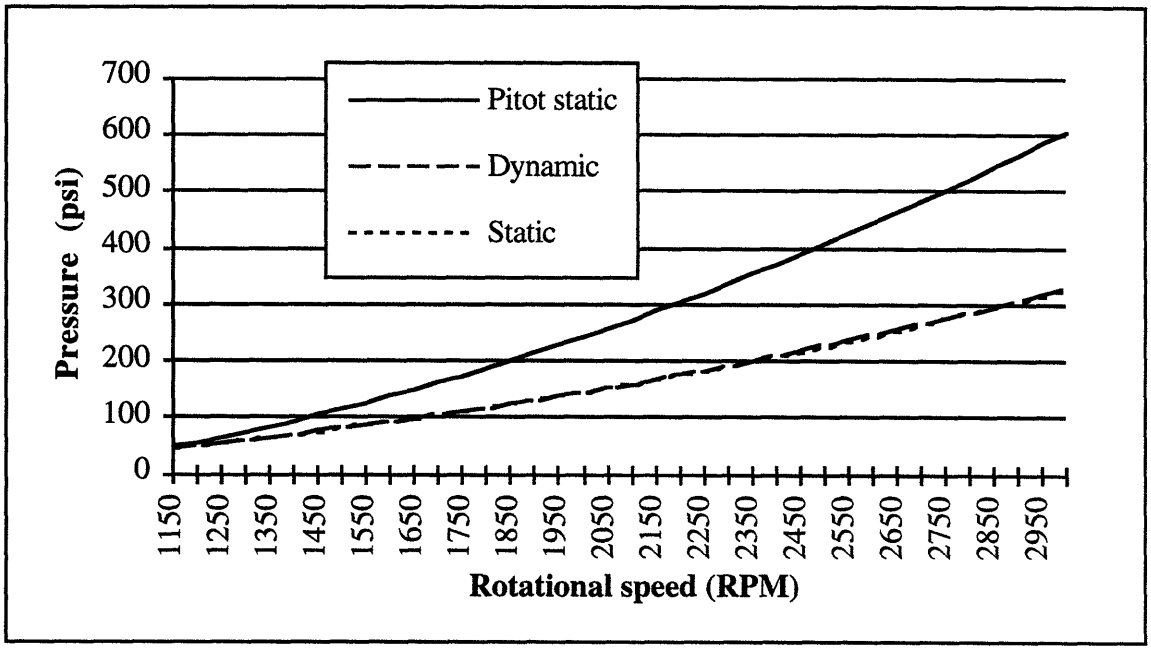

Figure 20: Influence of the rotational speed on the dynamic and static pressure contributions to the pitot pump (static) pressure. Here the pitot pump bowl is filled (l_S = *7.5"*) and the tube is 3/8" schedule 40 pipe.

4.4. Discussion of preliminary design results and recommendations

The concept of a centrifuge-pump seems proven performancewise, given that the pitot pump bowl, designed so that it can interface with an existing Bird Machine centrifuge processing 50 gpm, can generate 606 psi for a power output of 17.7 HP, neglecting losses due to the right-angle bends and wall friction. In reality, there will be significant losses as the high speed flow jets through the pitot tube. To reduce those losses, the high speed flow will have to be diffused as soon as possible after it enters the pitot tube. In other words, the dynamic flow energy ought to be transformed into useful potential pump energy, before the dynamic energy can dissipate due to the wall friction and the right-angle bends. There is therefore an incentive to design the pitot tube so that it gradually expands outwards, as the flow goes down it. There is a trade-off, however, since the external drag increases as the pitot tube is made wider. Thus, future computational work is needed to optimize the pitot tube diffusion length and divergence angle to achieve minimal internal losses, while minimizing external drag forces on the pitot tube.

External drag on the tube can be greatly reduced by using a different pitot tube geometry. While the drag force of 466 lb is unusually high for a 3/8" schedule 40 pitot tube, an airfoil-shaped tube can reduce the drag force by two orders of magnitude, as discussed. Further, appropriate selection of tube material and manufacturing process for fabricating the tube and exit pipe coaxial with the feed pipe (as shown in **Figure 8**), will ensure that the tube will resist yield at the joint to the exit pipe.

Another important parameter to consider is the width of the pitot pump bowl. Typically the width is chosen to minimize interference drag; it is on the order of several pitot tube diameters in practice[3]. The pitot pump bowl therefore has a very small width

[3]Kent Weber, author of several recent pitot pump patents assigned to Sundstrand Corporation, was kind enough to provide this information based on his experience.

compared to its diameter. Interference drag consists of a combination of pitot tube wake drag and bowl wall friction drag. Analytical tools to predict the optimal pitot pump bowl width are unavailable at present[4]. This is partly due to the fact that the pitot pump is a rather obscure pump that has not found widespread use as yet. Since the pitot pump bowl width is so small compared to the bowl diameter and cannot be predicted from analysis as yet, it was reasonable to neglect it in the analysis here.

---

[4]Ibid.

5. Retrofitting the pitot pump bowl to a decanter-type centrifuge

Now that the concept is proven performancewise, it is important to determine how the pitot pump bowl can be successfully retrofitted to an existing decanter-type centrifuge. This chapter explains the challenges involved, and presents a solution which includes novel design features.

Figure 21 shows a cross-section of a Bird Machine decanter-type centrifuge, obtained from Bird Machine's most recent patent on a decanter-type centrifuge [5]. A 2-D cross-section provides sufficient information, to determine how to configure the pitot pump bowl. Here, the two primary objectives were as follows:

1. Configuration of the pitot pump bowl so that the centrate can enter at the pitot pump bowl inner radius, and be accelerated to maximum tangential velocity , with minimal changes in the design of the decanter-type centrifuge.

2. Configuration of the pitot pump bowl so that the centrate can be pumped out, also with minimal changes in the design of the decanter-type centrifuge.

To accomplish accelerated entry into the pitot pump bowl, the fluid emerging from the weirs of the centrifuge bowl can be channeled to the inner radius of the pitot pump bowl, by fastening a circular manifold onto the centrifuge bowl, as shown in **Figure 8**. The tangential velocity of the fluid entering the pump bowl is already close to 100% of the pump bowl inner radius tangential velocity, since the entering fluid has approximately the same tangential velocity as the centrifuge bowl inner radius tangential velocity. By the time the fluid gets past the manifold, it is approximately at 100 % of the pump bowl inner radius tangential velocity.

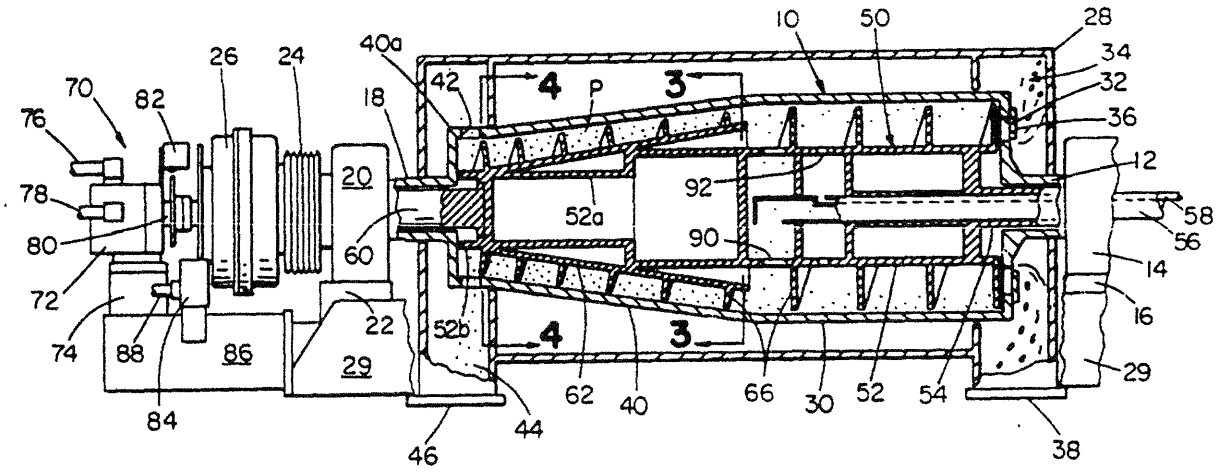

Figure 21: Cross-section of a Bird Machine Company decanter-type centrifuge obtained from Bird Machine Company's most recent patent (U. S. patent no. 4,381,849)

Configuring the pitot pump bowl so that the centrate can be pumped out, without having to significantly alter the design of the decanter centrifuge, is a more difficult challenge. To understand this challenge, it is instructive to examine **Figure 21**. Here the discussion will focus on the design changes that need to be made in the decanter-type centrifuge to accommodate the pitot pump, rather than on the description of the function of each numbered part of the centrifuge. Complete details on the function of each component can be found in the patent (U. S. patent no. 4,381,849). The rotating bowl has sleeve shafts **18** and **12** at either end, rotatable on bearing mounts **20** and **14**, respectively. The challenge is to channel the fluid from the pitot tube through a conduit coaxial with the feed pipe **56**. This is the only way that the pumped fluid can exit from the spinning bowl.

Fortunately, this can be accomplished with little design changes in an existing decanter centrifuge of the type shown in **Figure 21**. The advantage of this decanter centrifuge design, is that both the drive pulley **24** and the gear box **26** are mounted on the left side; this leaves the right side with essentially only a bearing mount **14** and a stationary feed pipe **56**. If somehow the pitot tube fluid could be channeled through a

conduit coaxial with the stationary feed pipe to the outside, this conduit could be conveniently connected to a pipe or hose going to the hydrostatic bearings, since there is no gear box or drive pulley in the way.

Figure 22 shows the proposed design for the integrated decanter-type centrifuge-pitot pump. The pitot pump bowl diameter can be selected to achieve the desired pump pressure. Referring back to **Figure 21**, one sees that the conveyor shaft **60**, which rotates at a differential speed with respect to the rotating bowl **10**, is shortened on the right side in **Figure 22**, so that it does not protrude into the pitot pump bowl **1**. With the conveyor shaft **7** shortened, the stationary feed pipe **2** is the only protrusion into the pitot pump bowl **1**. A stationary pipe channeling the pumped fluid out **3** can be fastened onto the outside of the feed pipe **2** so that it is concentric to the feed pipe **2**, as shown in **Figure 22**. The pitot pump bowl **1** is fastened onto the centrifuge bowl **4** on one side, and onto a sleeve shaft **5** on the other, forming a contiguous bowl assembly. The sleeve shaft envelopes both the feed pipe **2** and the discharge pipe **3**.

A needle roller bearing **6** is mounted between the end of the conveyor sleeve shaft **7** and the bowl assembly shaft **8**. The needle roller bearing **6** permits differential motion between the conveyor **9** and the bowl assembly. At the right end, the bowl assembly sleeve shaft **5** is supported by a heavy-duty straight roller bearing **10**. A spherical roller bearing could also be used instead, to minimize alignment sensitivity.

To prevent fluid from leaking out of the pitot pump bowl **1**, seals are needed between the conveyor sleeve shaft **7** and the feed pipe **2**, and between the bowl assembly sleeve shaft **5** and the discharge pipe **3**. A visco seal has been proposed as the seal at both locations. The visco seal is used to seal liquids or gases in rotating shaft equipment. The visco seal has found tremendous success as a seal in machine tool hydrostatic spindles. It offers the combination of zero leakage, long life and reliability [6]. This seal is schematically shown as a jagged edge **11** in **Figure 22**. **Figure 23** illustrates a visco seal in detail [7].

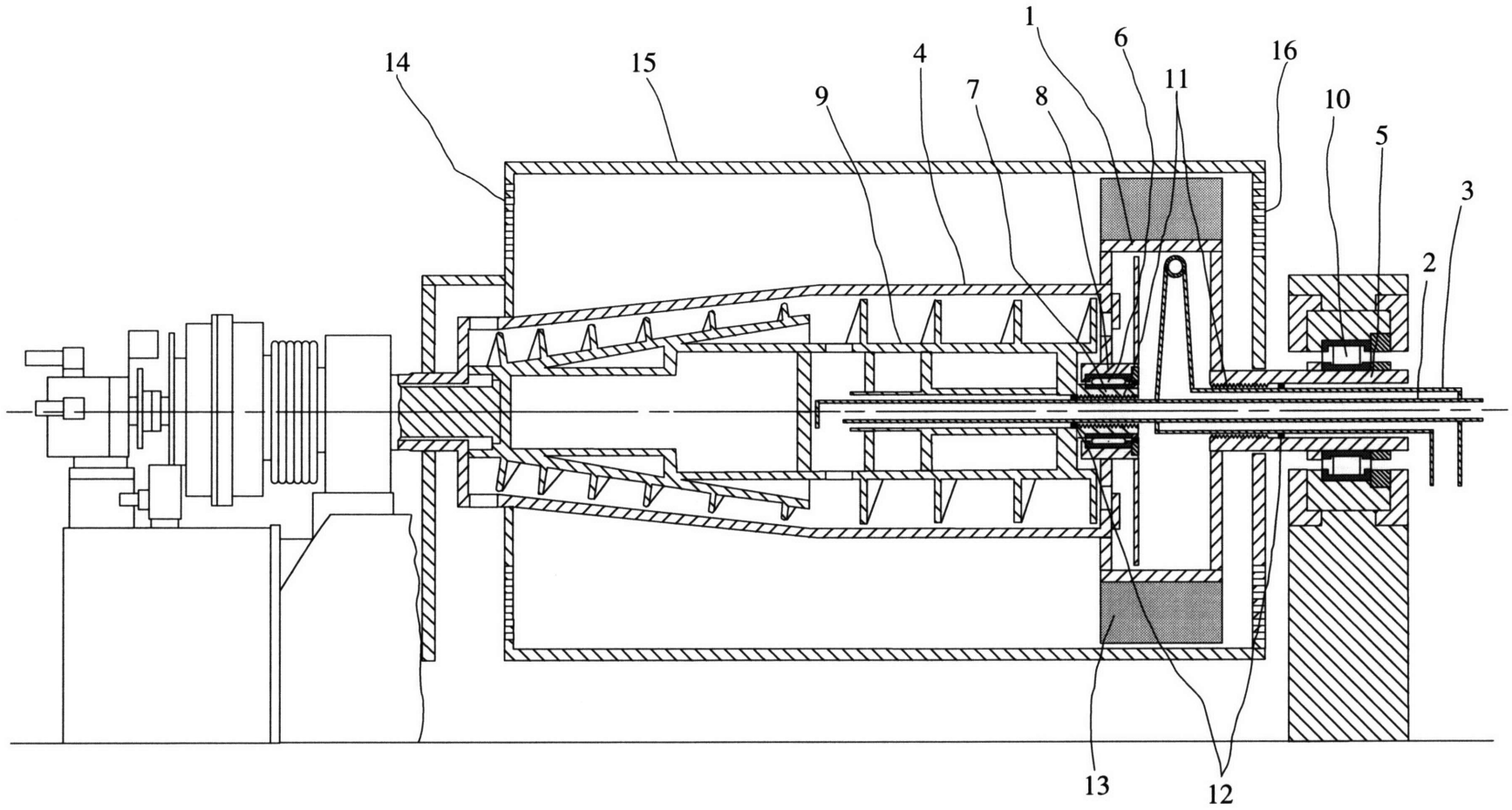

Figure 22: Cross-section of the integrated decanter-type centrifuge-pitot pump developed in this thesis: 1 - pitot pump bowl; 2 - feed pipe; 3 - discharge pipe; 4 - centrifuge bowl; 5 - sleeve shaft; 6 - needle roller bearing; 7 - conveyor sleeve shaft; 8 - bowl assembly shaft; 9 - conveyor; 10 - straight roller bearing; 11 - visco seal; 12 - lip seal; 13 - fan blading; 14 - air inlet holes; 15 - blow-proof housing; 16 - air exit holes

To seal the system fluid, the visco seal relies on the screw-pumping action of a viscous fluid in the clearance gap between the bore and the shaft. The pumping action is created by the relative motion between the bore and the shaft. A viscous liquid is fed into the clearance gap through an orifice, as shown in **Figure 23**. On the left side of the orifice, the shaft has a right hand thread, so that the viscous fluid is pumped against the system fluid (in this case, the pitot pump bowl fluid). On the right side of the orifice, the shaft has a left-hand thread, which causes the viscous fluid to be pumped away from the system fluid. The two screw pumps pump against each other, producing an axial pressure gradient on either side of the orifice, resulting in essentially zero flow [7]. The helical grooves may be machined either onto the shaft, or in a sleeve that is inserted into the bore (threaded sleeve).

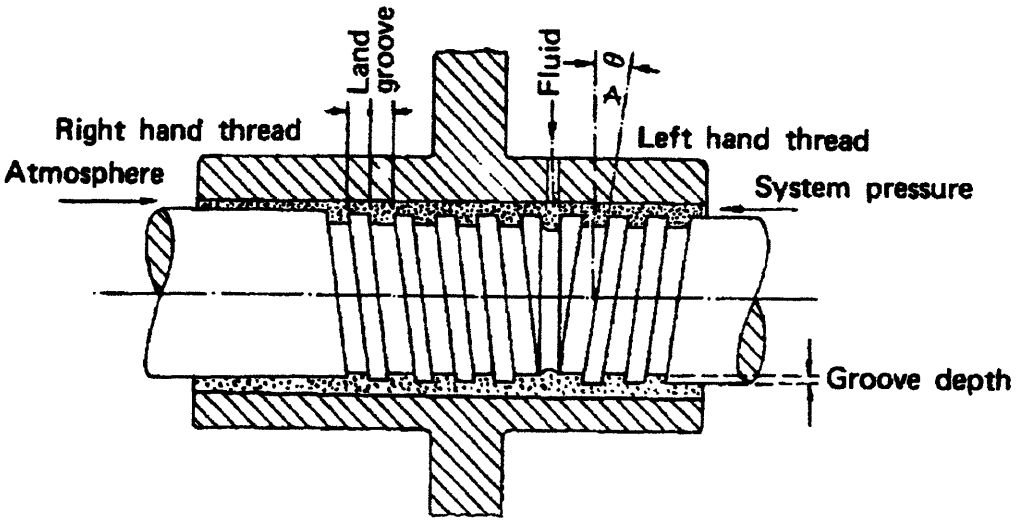

Figure 23: A visco seal where the shaft has the threads

In the centrifuge-pump shown in **Figure 22,** threaded sleeves **11** are fitted in the rotating bores at both seal locations. Alternatively, the helical grooves could be machined onto the stationary feed pipe **2** and discharge pipe **3** if this proves to be simpler. A conduit coaxial with the feed pipe **2** and the discharge pipe **3** (not shown in **Figure 22**), provides the viscous sealing fluid to the clearance gaps at both seals. To prevent leakage

once the bowl assembly stops rotating, lip seals **12** are provided at the ends of the visco seals. The lip seal contacts the threaded sleeve once the bowl assembly stops rotating. During rotation, the centrifugal force prevents the lip seal from contacting the threaded sleeve [7].

Enhanced heat removal is another novel feature, made possible by retrofitting the pitot pump bowl to a decanter-type centrifuge. With the addition of fan blades **13** to the curved exterior of the pitot pump bowl **1**, the assembly transforms into a more effective heat exchanger. Fan blades **13** fastened onto the rotating bowl entrain ambient air through holes **14** in the blow-proof housing **15** on the centrifuge end, and channel the air through exit holes **16** on the pump end. The motivation for having the air flow from the centrifuge bowl end to the pitot pump bowl end, is that the temperature gradient is expected to be towards the pitot pump bowl end, since the pitot pump bowl is expected to be hotter than the centrifuge bowl due to pitot tube drag energy dissipation. Thus it is sensible to blow the hot air surrounding the pitot pump bowl out, and replace it with cooler air coming from the centrifuge end. The cooling air increases convective heat transfer along the axial extent of the centrifuge bowl **4**. Further, the fan blades **13** also enhance heat transfer from the pitot pump bowl **1**, by acting as fins.

6. Conclusion

The initial goal of this thesis was to focus on designing the filtration component of the support equipment for a precision machine tool employing self-compensating hydrostatic bearings. There was an immediate need for a low-cost, self-cleaning separator dedicated to removing low specific gravity ceramic fines from water-based coolant. A thorough survey was conducted and it was found that other conventional (for metallic fines) filters and separators also proved ineffective at filtering out low specific gravity ceramic fines cost-effectively. Centrifugal separation was found to be the best means towards removing such fines, and a low-cost centrifuge design with the top open to atmospheric pressure was initially pursued. Containing the centrate proved to be difficult, and motivated a careful examination of existing automatic, self-cleaning centrifuge technology. This led to a new integrated decanter-type centrifuge-pitot pump design which not only accomplishes the required filtration, but also generates the high pressure, pulsation-free flow required by hydrostatic bearings for precision machine tools and is self-cooling.

Calculations were performed that indicate that the centrifuge-pitot pump can provide the high pumping pressure required for a hydrostatic machine tool system in a compact bowl. The pump bowl can be retrofitted onto an existing decanter-type centrifuge without major re-design of the centrifuge. The novel design features offered by the centrifuge-pitot pump have motivated the filing for a patent on the concept.

In the context of the initial goal of this thesis, which was to develop a job-shop affordable, self-cleaning separator for removing ceramic fines, it is clear that an integrated decanter-type centrifuge-pitot pump is too costly to be the separator sought. However, for the job shop that intends to use machine tools that use self-compensating hydrostatic bearings, a high performance pump together with a hassle-free, reliable and robust filtration system is as important an investment as the hydrostatic machine tool

itself, since the support equipment is an integral part of the hydrostatic machine tool system. The integrated decanter-type centrifuge-pitot pump is two in one: one obtains both a high pressure pump and a decanter-type centrifuge for the cost of the decanter-type centrifuge. This is another great advantage. Furthermore, the addition of the fan-bladed pitot pump bowl transforms the assembly into an effective heat exchanger.

Indeed, the centrifuge-pitot pump has the potential to be developed into a commercial product. Its market would include applications where slurry needs to be clarified and undergo high pressure pumping. As such, the design needs to go through the later stages of product development. Now that the concept is proven analytically and schematically, the next stage is to develop detail drawings for a pilot-scale prototype. Close interaction with a centrifuge manufacturer, and if possible, a pitot pump supplier would be necessary at this stage.

References

1. Slocum, A. H., Scagnetti, P. A., Kane, N. R., and Brunner, C., "Design of self-compensated, water-hydrostatic bearings," *Precision Engineering*, vol. 17, no. 3, July 1995, pp. 173-185

2. Ashley, S., "Building a better bearing," *Mechanical Engineering*," vol. 118, no. 5, May 1996, pp. 56-60

3. Schlichting, H., *Boundary Layer Theory* (7th ed.), McGraw-Hill, New York, 1977

4. Abbott, I. H., and von Doenhoff, A. E., *Theory of Wing Sections*, Dover Books, New York, 1959

5. Conant, L. D., *Solids-Liquid Slurry Separating Centrifuge*, U. S. Patent # 4,381,849, assigned to Bird Machine Company, May 3, 1983

6. Stair, W. K., "Effect of Groove Geometry on Viscoseal Performance," *Journal of Engineering for Power, Transactions of the American Society of Mechanical Engineers*, vol. 89, October 1967, pp. 605-614

7. Buchter, H. H., *Industrial Sealing Technology*, John Wiley and Sons, New York, 1979

Appendix A: Understanding the parameters that affect filtration

Filtration is a science in itself, and in order to specify the right filter or separator, one must first thoroughly understand filtration terminology, and the criteria for selecting filters. Appendix A summarizes important terms and filter selection criteria used in the filtration industry. Performance measures and costs of batch-type centrifuges are discussed in Appendix B.

Filtration efficiency, beta ratios, dirt-holding capacity, and pressure requirements are the principal filter selection criteria. These criteria are mainly governed by seven parameters in water-based coolant emulsions: flow rate, ingestion rate, geometry of the particles being filtered, particle specific gravity, particle size distribution, filter element loading, and contaminant leakage rate across bypass valves and housing-element interfaces. Unfortunately for the end-users, all of these parameters tend to be unique, differing from one application to another. Thus filtration efficiencies, beta ratios and dirt-holding capacities specified by filter manufacturers can often be misleading, because they are determined using a completely different set of parameters than those in field conditions. It is instructive to understand how each of these parameters affects the filter's performance.

1. Flow rate

Regardless of the type of filter, the filter's efficiency will scale inversely with the flow rate. As the flow rate decreases, the dwell time of a particle in the filter increases, allowing more time for the particle to be trapped.

In the case of media-type filters, the nature of the flow also affects filter performance. The filter's efficiency reported for a steady flow will be different than the same filter's efficiency reported for a pulsating flow. Pulsating or cyclic flows lead to

lower efficiencies. When the flow pulsates, finer particles that are ordinarily trapped by larger uneven particles caught in the media, are forced through the media. This is analogous to a sieve holding different size pebbles, some of which are smaller than the screen mesh [8]. When the sieve is shaken, some of the smaller pebbles that were caught between the bigger pebbles sift through.

2. Ingestion rate

Contaminants originate from three primary sources: built-in, ingressed, and wear-induced. Built-in contaminants include particles that are left behind after fabrication, such as metal chips. Ingressed contaminants include particles that enter the stream from the external environment, such as from the air, breathers and seals. Wear-induced contaminants are particles that emerge as a result of internal wear.

For media-type filters, the rate at which these contaminants enter the stream affects the filter's efficiency. If the contaminants enter in small concentrations, particles smaller than the mean pore size will readily pass through the filter. On the other hand if contaminants enter in high concentrations, particles will tend to clump up at the filter, and prevent particles smaller than the mean pore size from passing.

3. Particle geometry

Particle geometry influences the performance of media-type filters. Irregularly shaped particles have crevices which can get wedged into the filter media, and wedge into other particles already trapped. Thus, particles that are irregularly shaped will get caught more easily than particles that are smooth, and spherically shaped.

4. Particle density

The density of a particle influences the settling velocity of the particle. For cyclonic filters and centrifuges, density is a critical parameter. Particles with low densities will tend to take a long time to settle, and will be less amenable to cyclonic filtration. This can be seen by examining the Stoke's flow equation for settling velocity (*Vf*) of a spherical particle in a fluid for which the Reynolds number is sufficiently small for free fall to occur :

$$V_f = \frac{(\rho_p - \rho_f) g D^2}{18\mu} \qquad (A.1)$$

where ρ_p is the density of the particle, ρ_f is the density of the fluid, g is the acceleration due to gravity, D is the diameter of the particle, and μ is the viscosity of the fluid. From this equation, the following conclusions can be made:

1. The settling velocity is directly proportional to the difference in densities between the particle and the fluid. The greater the difference between the particle density and the fluid density, the larger the settling velocity.

2. The settling velocity is proportional to the square of the particle's diameter. Thus the larger the particle diameter, the greater the settling velocity.

3. The settling velocity is inversely proportional to the fluid viscosity. Thus as the fluid becomes less viscous, the settling velocity increases.

In a settling tank, the settling velocity time computed from (*A.1*) will be a good indication of how long it will take to separate out a particle. However in a basket-type

centrifuge, the centripetal acceleration is typically in excess of 1000 gravities, which greatly enhances separation.

5. Particle size distribution

For media-type filters, the presence of particles larger than the mean pore size will facilitate the capture of particles smaller than the mean pore size. Large particles getting caught in the filter media, act as an added barrier to incoming small particles. Thus a filter will be more efficient in trapping a distribution of particles varying in size, than trapping a distribution of small particles uniform in size.

6. Leakage rate across valves and seals

When the pressure drop across the filter element is excessive, or when there is a sudden surge in flow, it is common to have leakage across the housing-element seals, or across a bypass valve. In field situations, 1-2 % leakage flow is a real possibility. For 1% leakage, the maximum cumulative efficiency is limited to 99%, while for 2% leakage, maximum efficiency is limited to 98%. Thus leakage across the bypass and housing-element interface limits fine filtering performance.

7. Element loading

For a media-type filter, as the element becomes loaded, its efficiency changes. Usually when the element is new, the relative efficiency will be at a minimum, but will increase with element loading up to a certain point. This arises because as particles collect at the filter, they act as an added barrier to upstream particles. Beyond this point, the pressure drop increases dramatically, and the element has to be replaced.

For centrifuges, as the bowl gets filled with sludge, the number of gravities at which the particles are accelerated out changes. When the bowl is empty, particles are separated out at maximum centripetal acceleration, leading to maximum separation

efficiency. However as the bowl becomes filled, the number of gravities the particles are subjected to decreases, and hence the filtration efficiency decreases.

A.1 How filter suppliers determine efficiencies for their filters

Given that a filter or separator's performance is a function of the parameters above, which vary from application to application, filter specifications provided by manufacturers can rarely be applied to in-field situations. However tests and ratings have been developed for the sole purpose of comparing filters. It is important to understand how filter manufacturers specify their performance measures.

Filter manufacturers usually specify nominal ratings for their filters. Specifications MIL-F-5504A and MIL-F-5504B were established for determining nominal ratings [8]. Version A defines a 10 micrometer nominal filter as being able to remove 98% by weight of AC fine test dust particles larger than 10 micrometers at a certain high concentration. Version B defines a 10 micrometer nominal filter as being able to remove 95% by weight of glass beads 10-20 micrometers in size at a certain high concentration.

These standards have major limitations. First of all, there is no limitation on the maximum size particle allowed to pass through the filter. Tests have shown that some filters meeting these requirements can allow particles up to 200 micrometers to pass [8]. Further, many engineers fail to realize that 2-5% of particles by weight in production grinding streams is a dangerously high amount of contaminants.

Another efficiency rating which is commonly used, is the beta ratio. Here the manufacturer uses a test known as a multi-pass filter test, in which contaminant is continually ingested into a closed loop, recirculating test system. Upstream and downstream concentrations of the contaminant are monitored. A steady state level of

contaminants remaining in circulation is reached, and the beta ratio (β_μ) is expressed by the following equation:

$$\beta_\mu = \frac{1}{1 - E_\mu} \qquad (A.2)$$

where E_μ is the cumulative removal efficiency. The beta ratio has a nonlinear relation with efficiency, as shown in **Figure A.1**. Thus a filter having a beta ratio of 1000, compared to one having a beta ratio of 100, does not mean that the former is ten times better than the latter. A beta ratio of 1000 corresponds to 99.9 % efficiency, and a beta ratio of 100 corresponds to 99 % efficiency.

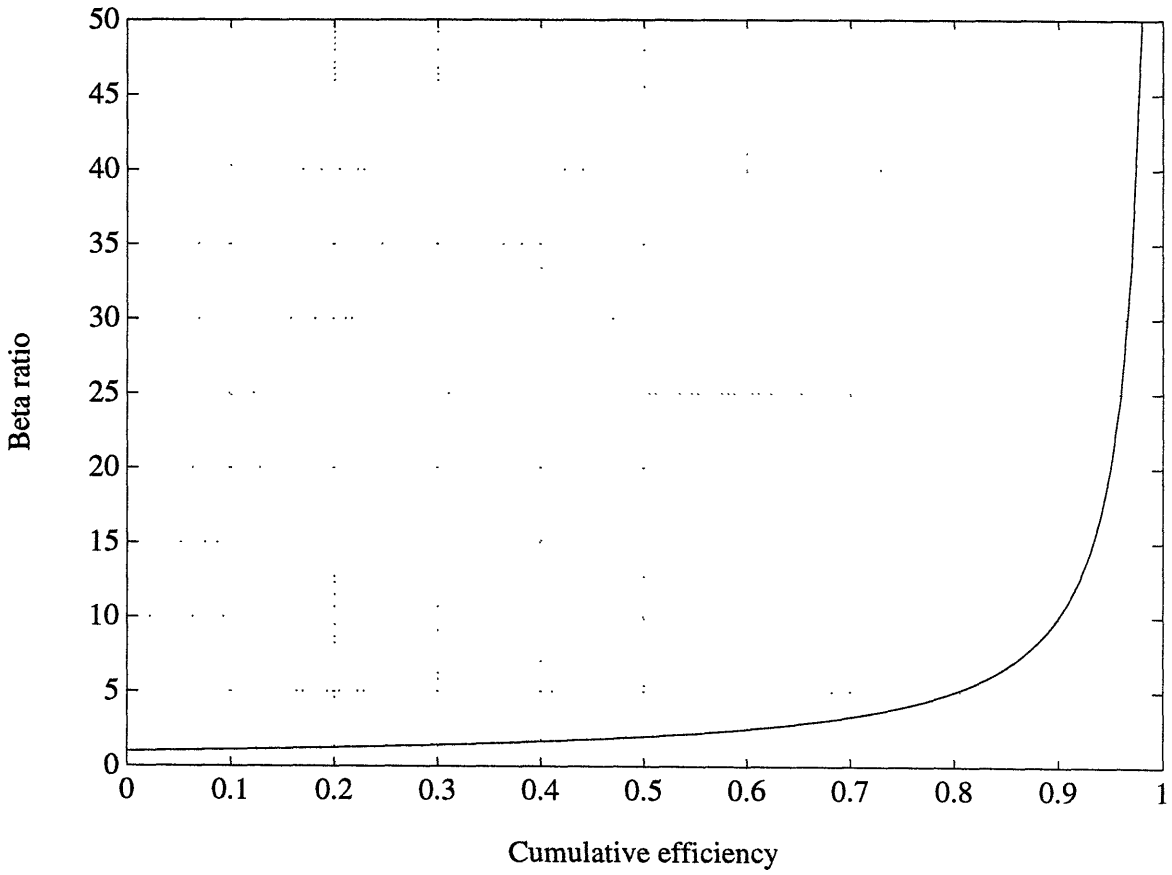

Figure A.1: Graph showing non-linear relationship between the Beta ratio and the cumulative efficiency

Here again, one must realize that the operational parameters used in the multi-pass filter test such as flow rate, ingestion rate, particle geometry, and so forth are selected to obtain repeatable test results, and tend to be entirely different from operational parameters in field situations. Therefore it is unwise to expect the filter to achieve the beta-rated performance for the user's application.

For tests to determine the nominal rating using MIL standards, and for the multi-pass filter test, the selection of two important operational parameters, flow rate, and degree of element loading are left up to the manufacturer to decide. Thus manufacturers can tailor the flow rate, and degree of element loading to yield the most favorable efficiency ratings. For this reason, it is important to ask manufacturers to provide the values of all the operational parameters used to obtain the filter efficiencies they report.

Perhaps a more informative filter selection criterion, but one that manufacturers often don't measure, is the absolute micron rating, which is defined according to the NFPA Fluid Power Glossary of Terms as the being the diameter of the largest hard spherical particle that will pass through a filter under specified test conditions [8]. This rating is a measure of the order of magnitude of the larger pores in a media-type filter. Because the operational parameters for determining the absolute micron rating of a filter, are likely to be different from the operational parameters in field situations, one still cannot expect the rating to apply to one's application. However the absolute micron rating is a good standard to compare filters.

Appendix B: Batch-type centrifuge survey

To compare the performance and costs of different batch-type centrifuges available, spreadsheets were made showing costs, necessary support equipment, and important specifications. In regards to the spreadsheet information, the following ought to be noted:

- Costs are approximate estimates obtained over the telephone.

- The centripetal acceleration values, are manufacturer specifications, and it is unclear under what conditions they were determined. It should be noted that maximum centripetal acceleration is not a good selection criterion. Manufacturers can increase the centripetal acceleration of the centrifuge to a certain limit (dictated by bowl material strength constraints), by changing the motor to a higher RPM.

- The interval of replacement of the manually removable bowl or liner was calculated assuming continuous grinding of ceramic at a removal rate of 0.05 cubic inches per minute[5], or 3 cubic inches per hour using the following simplified relation:

$$t = \frac{CAP}{2MRR} \qquad (B.1)$$

where t is the replacement interval in hours, CAP is the capacity of the removable centrifuge bowl or liner in cubic inches, and MRR is the material removal rate in

[5]Maximum removal rate in ceramic grinding at Weldon Machine Tool, Inc.

cubic inches per hour. To remain conservative, a safety factor of two was applied to the actual bowl/liner capacity to obtain the accommodated sludge capacity.

Manufacturer	Barrett centrifuges (U.S.)	Clinton Separators Inc (U.S)
Maximum flow rate (gpm)	15	16
Centrifuge		
Model Number	236	CS9021
Outer Dimensions (L x W x H)	28.63" x 20" x 18.13"	22.25" x 22.25" x 23.25"
Power consumption (HP)	3	2
Centrifuge bowl		
Volume (cubic in)	462	377
Replacement interval (hours)	77.0	62.8
Residence time for 5 gpm flow (s)	24.0	19.6
Performance		
Centripetal acceleration (G)	1000+	2600
Costs		
Cost of centrifuge	$6,000	$4,700
Cost of replaceable bowl		$1,500
Cost of replaceable liner	NOT AVAILABLE	NOT AVAILABLE
Support equipment		
Desc. and cost		
Desc. and cost		
Desc. and cost		
Desc. and cost		

Manufacturer	FSP (U.K)	Lavin (U.S.)
Maximum flow rate (gpm)	20	12
Centrifuge		
Model Number	FSP-1205-60G	12-413V
Outer Dimensions (L x W x H)	48" x 36" x 40"	24" x 24" x 24"
Power consumption (HP)	1.5	
Centrifuge bowl		
Volume (cubic in)	500	413
Replacement interval (hours)	83.3	68.8
Residence time for 5 gpm flow (s)	26.0	21.5
Performance		
Centripetal acceleration (G)	1150+	2200
Costs		
Cost of centrifuge	$11,000	$6,563
Cost of replaceable bowl		$1,316
Cost of replaceable liner	$195	NOT AVAILABLE
Support equipment		
Desc. and cost	60 gal tank included	diffuser @ $341 optional
Desc. and cost	lift pump included	anti-wave device @ $396 option.
Desc. and cost	clean fluid return pump included	
Desc. and cost	control panel @ $3,000 optional	

Manufacturer	Toto (Japan)	US Centrifuge
Maximum flow rate (gpm)	13	10
Centrifuge		
Model Number	TSK-50M	M212
Outer Dimensions (L x W x H)	26" x 15" x 20"	38" x 17" x 41"
Power consumption (HP)	2	3
Centrifuge bowl		
Volume (cubic cm)	415.8	498
Replacement interval (hours)	69.3	83.0
Residence time for 5 gpm flow (s)	21.6	25.9
Performance		
Centripetal acceleration (G)	1000+	2000
Costs		
Cost of machine	$6,000	$7,000
Cost of replaceable bowl		
Cost of replaceable liner	$200	$8
Support equipment		
Desc. and cost	3 hp starter @ $600 optional	Moino pos. disp. pump included
Desc. and cost		motor starter included
Desc. and cost		

Additional references

8. Gay, R. F., "Understanding hydraulic filter tests," *Hydraulics & Pneumatics,* February 1988

9. Vijlee, A., "Multipass Filter Test Masks Actual Performance," *Machine Design,* April 23, 1987

10. Drennen, J., "Shooting Holes in Filtration Myths," *Machine Design,* February 11, 1988